

# 4

## *Crystal Lattices*

Bravais Lattice and Primitive Vectors

Simple, Body-Centered, and Face-Centered  
Cubic Lattices

Primitive Unit Cell, Wigner-Seitz Cell, and  
Conventional Cell

Crystal Structures and Lattices with Bases

Hexagonal Close-Packed and Diamond Structures

Sodium Chloride, Cesium Chloride, and  
Zincblende Structures

Those who have not wandered amidst the mineralogical departments of natural history museums are often surprised to learn that metals, like most other solids, are crystalline, for although one is used to the very obvious crystalline features of quartz, diamond, and rock salt, the characteristic plane faces at sharp angles with one another are absent from metals in their most commonly encountered forms. However, those metals that occur naturally in the metallic state are quite often found in crystalline forms, which are completely disguised in finished metal products by the great malleability of metals, which permits them to be fashioned into whatever macroscopic shape one wishes.

The true test of crystallinity is not the superficial appearance of a large specimen, but whether on the microscopic level the ions are arranged in a periodic array.<sup>1</sup> This underlying microscopic regularity of crystalline matter was long hypothesized as the obvious way to account for the simple geometric regularities of macroscopic crystals, in which plane faces make only certain definite angles with each other. It received direct experimental confirmation in 1913 through the work of W. and L. Bragg, who founded the subject of X-ray crystallography and began the investigation of how atoms are arranged in solids.

Before we describe how the microscopic structure of solids is determined by X-ray diffraction and how the periodic structures so revealed affect fundamental physical properties, it is useful to survey some of the most important geometrical properties of periodic arrays in three-dimensional space. These purely geometrical considerations are implicit in almost all the analysis one encounters throughout solid state physics, and shall be pursued in this chapter and in Chapters 5 and 7. The first of many applications of these concepts will be made to X-ray diffraction in Chapter 6.

## BRAVAIS LATTICE

A fundamental concept in the description of any crystalline solid is that of the *Bravais lattice*, which specifies the periodic array in which the repeated units of the crystal are arranged. The units themselves may be single atoms, groups of atoms, molecules, ions, etc., but the Bravais lattice summarizes only the geometry of the underlying periodic structure, regardless of what the actual units may be. We give two equivalent definitions of a Bravais lattice<sup>2</sup>:

- (a) A Bravais lattice is an infinite array of discrete points with an arrangement and orientation that appears *exactly* the same, from whichever of the points the array is viewed.
- (b) A (three-dimensional) Bravais lattice consists of all points with position vectors  $\mathbf{R}$  of the form

$$\mathbf{R} = n_1\mathbf{a}_1 + n_2\mathbf{a}_2 + n_3\mathbf{a}_3, \quad (4.1)$$

---

<sup>1</sup> Often a specimen is made up of many small pieces, each large on the microscopic scale and containing large numbers of periodically arranged ions. This "polycrystalline" state is more commonly encountered than a single macroscopic crystal, in which the periodicity is perfect, extending through the entire specimen.

<sup>2</sup> Why the name Bravais appears is explained in Chapter 7.

where  $\mathbf{a}_1$ ,  $\mathbf{a}_2$ , and  $\mathbf{a}_3$  are any three vectors not all in the same plane, and  $n_1$ ,  $n_2$ , and  $n_3$  range through all integral values.<sup>3</sup> Thus the point  $\sum n_i \mathbf{a}_i$  is reached by moving  $n_i$  steps<sup>4</sup> of length  $a_i$  in the direction of  $\mathbf{a}_i$  for  $i = 1, 2$ , and 3.

The vectors  $\mathbf{a}_i$  appearing in definition (b) of a Bravais lattice are called *primitive vectors* and are said to *generate* or *span* the lattice.

It takes some thought to see that the two definitions of a Bravais lattice are equivalent. That any array satisfying (b) also satisfies (a) becomes evident as soon as both definitions are understood. The argument that *any* array satisfying definition (a) can be generated by an appropriate set of three vectors is not as obvious. The proof consists of an explicit recipe for constructing three primitive vectors. The construction is given in Problem 8a.

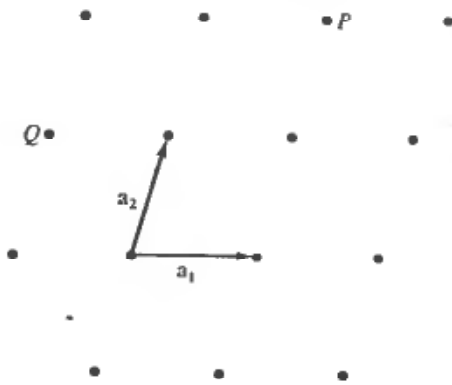


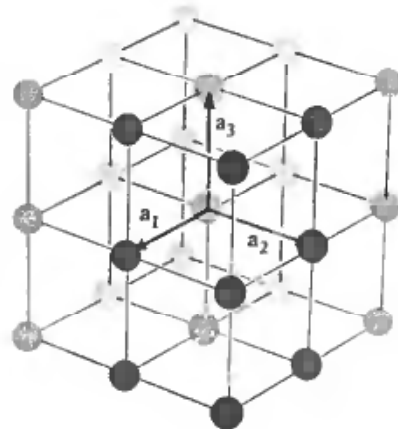
Figure 4.1

A general two-dimensional Bravais lattice of no particular symmetry: the oblique net. Primitive vectors  $\mathbf{a}_1$  and  $\mathbf{a}_2$  are shown. All points in the net are linear combinations of these with integral coefficients; for example,  $P = \mathbf{a}_1 + 2\mathbf{a}_2$ , and  $Q = -\mathbf{a}_1 + \mathbf{a}_2$ .

Figure 4.1 shows a portion of a two-dimensional Bravais lattice.<sup>5</sup> Clearly definition (a) is satisfied, and the primitive vectors  $\mathbf{a}_1$  and  $\mathbf{a}_2$  required by definition (b) are indicated in the figure. Figure 4.2 shows one of the most familiar of three-dimensional Bravais lattices, the simple cubic. It owes its special structure to the fact that it can be spanned by three mutually perpendicular primitive vectors of equal length.

Figure 4.2

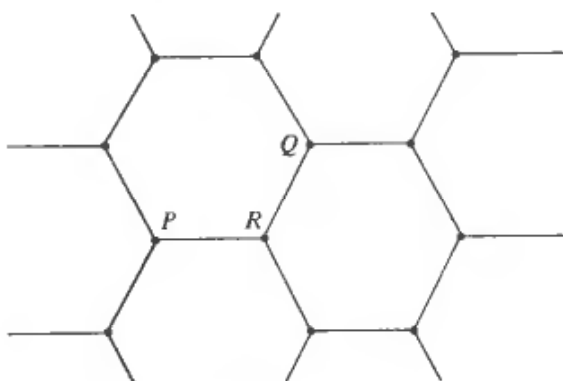
A simple cubic three-dimensional Bravais lattice. The three primitive vectors can be taken to be mutually perpendicular, and with a common magnitude.



<sup>3</sup> We continue with the convention that “integer” means a negative integer or zero, as well as a positive integer.

<sup>4</sup> When  $n$  is negative,  $n$  steps in a direction means  $n$  steps in the opposite direction. The point reached does not, of course, depend on the order in which the  $n_1 + n_2 + n_3$  steps are taken.

<sup>5</sup> A two-dimensional Bravais lattice is also known as a *net*.

**Figure 4.3**

The vertices of a two-dimensional honeycomb do *not* form a Bravais lattice. The array of points has the same appearance whether viewed from point *P* or point *Q*. However, the view from point *R* is rotated through  $180^\circ$ .

It is important that not only the arrangement, but also the orientation must appear the same from every point in a Bravais lattice. Consider the vertices of a two-dimensional honeycomb (Figure 4.3). The array of points looks the same when viewed from adjacent points only if the page is rotated through  $180^\circ$  each time one moves from one point to the next. Structural relations are clearly identical, but *not* orientational relations, so the vertices of a honeycomb do not form a Bravais lattice. A case of more practical interest, satisfying the structural but not the orientational requirements of definition (a), is the three-dimensional hexagonal close-packed lattice, described below.

## INFINITE LATTICES AND FINITE CRYSTALS

Since all points are equivalent, the Bravais lattice must be infinite in extent. Actual crystals are, of course, finite, but if they are large enough the vast majority of points will be so far from the surface as to be unaffected by its existence. The fiction of an infinite system is thus a very useful idealization. If surface effects are of interest the notion of a Bravais lattice is still relevant, but now one must think of the physical crystal as filling up only a finite portion of the ideal Bravais lattice.

Frequently one considers finite crystals, not because surface effects are important, but simply for conceptual convenience, just as in Chapter 2 we placed the electron gas in a cubical box of volume  $V = L^3$ . One then generally picks the finite region of the Bravais lattice to have the simplest possible form. Given three primitive vectors  $\mathbf{a}_1$ ,  $\mathbf{a}_2$ , and  $\mathbf{a}_3$ , one usually considers the finite lattice of  $N$  sites to be the set of points of the form  $\mathbf{R} = n_1\mathbf{a}_1 + n_2\mathbf{a}_2 + n_3\mathbf{a}_3$ , where  $0 \leq n_1 < N_1$ ,  $0 \leq n_2 < N_2$ ,  $0 \leq n_3 < N_3$ , and  $N = N_1N_2N_3$ . This artifact is closely connected with the generalization to the description of crystalline systems<sup>6</sup> of the periodic boundary condition we used in Chapter 2.

## FURTHER ILLUSTRATIONS AND IMPORTANT EXAMPLES

Of the two definitions of a Bravais lattice, definition (b) is mathematically more precise and is the obvious starting point for any analytic work. It has, however, two

<sup>6</sup> We shall make particular use of it in Chapters 8 and 22.

minor shortcomings. First, for any given Bravais lattice the set of primitive vectors is not unique—indeed, there are infinitely many nonequivalent choices (see Figure 4.4)—and it is distasteful (and sometimes misleading) to rely too heavily on a definition that emphasizes a particular choice. Second, when presented with a particular array of points one usually can tell at a glance whether the first definition is satisfied, although the existence of a set of primitive vectors or a proof that there is no such set can be rather more difficult to perceive immediately.

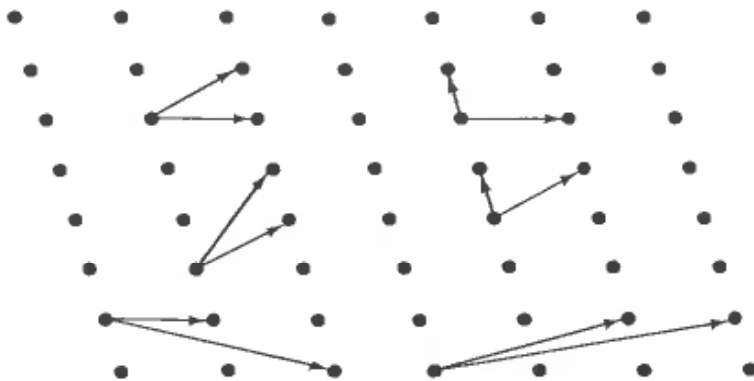
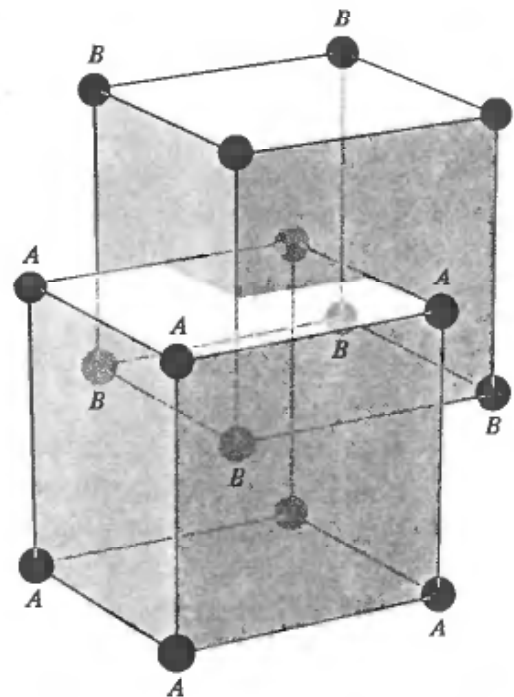


**Figure 4.4**  
Several possible choices of pairs of primitive vectors for a two-dimensional Bravais lattice. They are drawn, for clarity, from different origins.

Consider, for example, the *body-centered cubic* (bcc) lattice, formed by adding to the simple cubic lattice of Figure 4.2 (whose sites we now label *A*) an additional point, *B*, at the center of each little cube (Figure 4.5). One might at first feel that the center points *B* bear a different relation to the whole than the corner points *A*. However, the center point *B* can be thought of as corner points of a second simple cubic array.

**Figure 4.5**  
A few sites from a body-centered cubic Bravais lattice. Note that it can be regarded either as a simple cubic lattice formed from the points *A* with the points *B* at the cube centers, or as a simple cubic lattice formed from the points *B* with the points *A* at the cube centers. This observation establishes that it is indeed a Bravais lattice.



In this new array the corner points *A* of the original cubic array are center points. Thus all points do have identical surroundings, and the body-centered cubic lattice is a Bravais lattice. If the original simple cubic lattice is generated by primitive vectors

$$a\hat{x}, \quad a\hat{y}, \quad a\hat{z}, \quad (4.2)$$

where  $\hat{x}$ ,  $\hat{y}$ , and  $\hat{z}$  are three orthogonal unit vectors, then a set of primitive vectors for the body-centered cubic lattice could be (Figure 4.6)

$$\mathbf{a}_1 = a\hat{x}, \quad \mathbf{a}_2 = a\hat{y}, \quad \mathbf{a}_3 = \frac{a}{2}(\hat{x} + \hat{y} + \hat{z}). \quad (4.3)$$

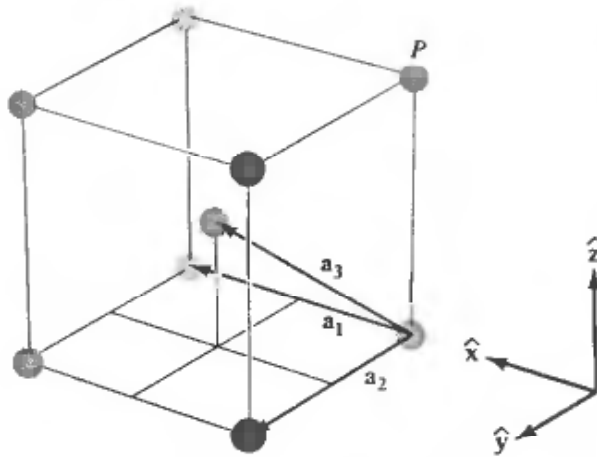


Figure 4.6

Three primitive vectors, specified in Eq. (4.3), for the body-centered cubic Bravais lattice. The lattice is formed by taking all linear combinations of the primitive vectors with integral coefficients. The point  $P$ , for example, is  $P = -\mathbf{a}_1 - \mathbf{a}_2 + 2\mathbf{a}_3$ .

A more symmetric set (see Figure 4.7) is

$$\mathbf{a}_1 = \frac{a}{2}(\hat{y} + \hat{z} - \hat{x}), \quad \mathbf{a}_2 = \frac{a}{2}(\hat{z} + \hat{x} - \hat{y}), \quad \mathbf{a}_3 = \frac{a}{2}(\hat{x} + \hat{y} - \hat{z}). \quad (4.4)$$

It is important to convince oneself both geometrically and analytically that these sets do indeed generate the bcc Bravais lattice.

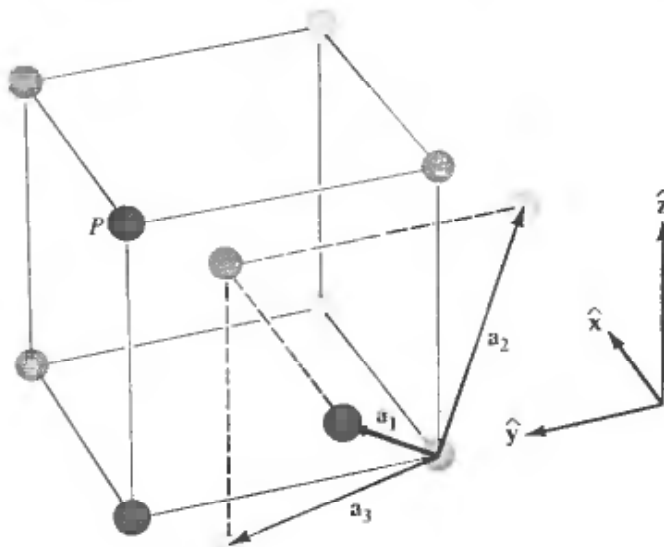


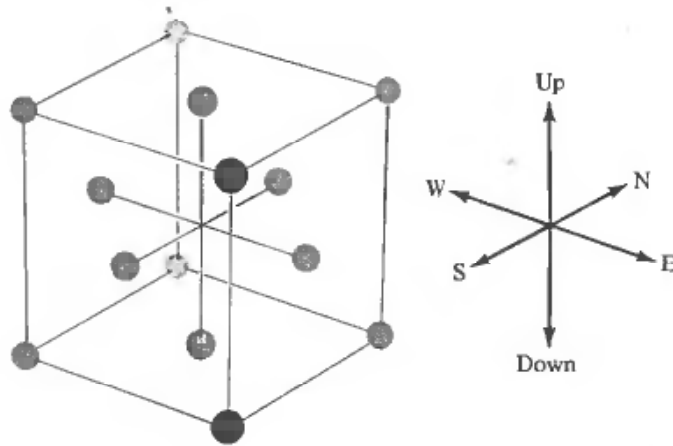
Figure 4.7

A more symmetric set of primitive vectors, specified in Eq. (4.4), for the body-centered cubic Bravais lattice. The point  $P$ , for example, has the form  $P = 2\mathbf{a}_1 + \mathbf{a}_2 + \mathbf{a}_3$ .

Another equally important example is the *face-centered cubic* (fcc) Bravais lattice. To construct the face-centered cubic Bravais lattice add to the simple cubic lattice of Figure 4.2 an additional point in the center of each square face (Figure 4.8). For ease in description think of each cube in the simple cubic lattice as having horizontal bottom and top faces, and four vertical side faces facing north, south, east, and west. It may sound as if all points in this new array are not equivalent, but in fact they are. One can, for example, consider the *new* simple cubic lattice formed by the points added

Figure 4.8

Some points from a face-centered cubic Bravais lattice.



to the centers of all the horizontal faces. The original simple cubic lattice points are now centering points on the horizontal faces of the new simple cubic lattice, whereas the points that were added to the centers of the north-south faces of the original cubic lattice are in the centers of the east-west faces of the new one, and vice versa.

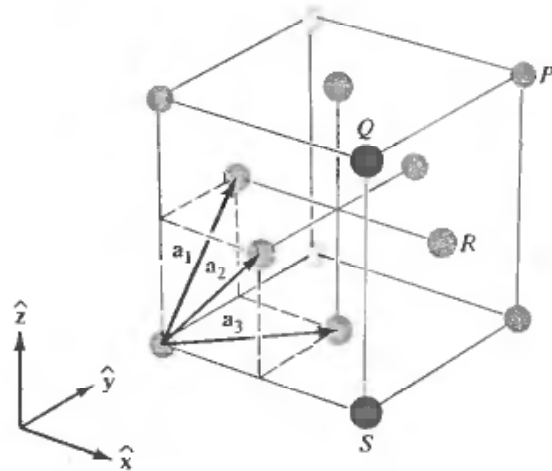
In the same way one can also regard the simple cubic lattice as being composed of all points centering the north-south faces of the original simple cubic lattice, or all points centering the east-west faces of the original cubic lattice. In either case the remaining points will be found centered on the faces of the new simple cubic framework. Thus any point can be thought of either as a corner point or as a face-centering point for any of the three kinds of faces, and the face-centered cubic lattice is indeed a Bravais lattice.

A symmetric set of primitive vectors for the face-centered cubic lattice (see Figure 4.9) is

$$\mathbf{a}_1 = \frac{a}{2}(\hat{y} + \hat{z}), \quad \mathbf{a}_2 = \frac{a}{2}(\hat{z} + \hat{x}), \quad \mathbf{a}_3 = \frac{a}{2}(\hat{x} + \hat{y}). \quad (4.5)$$

Figure 4.9

A set of primitive vectors, as given in Eq. (4.5), for the face-centered cubic Bravais lattice. The labeled points are  $P = \mathbf{a}_1 + \mathbf{a}_2 + \mathbf{a}_3$ ,  $Q = 2\mathbf{a}_2$ ,  $R = \mathbf{a}_2 + \mathbf{a}_3$ , and  $S = -\mathbf{a}_1 + \mathbf{a}_2 + \mathbf{a}_3$ .



The face-centered cubic and body-centered cubic Bravais lattices are of great importance, since an enormous variety of solids crystallize in these forms with an atom (or ion) at each lattice site (see Tables 4.1 and 4.2). (The corresponding simple cubic form, however, is very rare, the alpha phase of polonium being the only known example among the elements under normal conditions.)

Table 4.1  
ELEMENTS WITH THE MONATOMIC FACE-CENTERED  
CUBIC CRYSTAL STRUCTURE

ELEMENT	$a$ (Å)	ELEMENT	$a$ (Å)	ELEMENT	$a$ (Å)
Ar	5.26 (4.2 K)	Ir	3.84	Pt	3.92
Ag	4.09	Kr	5.72 (58 K)	$\delta$ -Pu	4.64
Al	4.05	La	5.30	Rh	3.80
Au	4.08	Ne	4.43 (4.2 K)	Sc	4.54
Ca	5.58	Ni	3.52	Sr	6.08
Ce	5.16	Pb	4.95	Th	5.08
$\beta$ -Co	3.55	Pd	3.89	Xe (58 K)	6.20
Cu	3.61	Pr	5.16	Yb	5.49

Data in Tables 4.1 to 4.7 are from R. W. G. Wyckoff, *Crystal Structures*, 2nd ed., Interscience, New York, 1963. In most cases, the data are taken at about room temperature and normal atmospheric pressure. For elements that exist in many forms the stable room temperature form (or forms) is given. For more detailed information, more precise lattice constants, and references, the Wyckoff work should be consulted.

Table 4.2  
ELEMENTS WITH THE MONATOMIC BODY-CENTERED  
CUBIC CRYSTAL STRUCTURE

ELEMENT	$a$ (Å)	ELEMENT	$a$ (Å)	ELEMENT	$a$ (Å)
Ba	5.02	Li	3.49 (78 K)	Ta	3.31
Cr	2.88	Mo	3.15	Tl	3.88
Cs	6.05 (78 K)	Na	4.23 (5 K)	V	3.02
Fe	2.87	Nb	3.30	W	3.16
K	5.23 (5 K)	Rb	5.59 (5 K)		

## A NOTE ON USAGE

Although we have defined the term “Bravais lattice” to apply to a set of points, it is also generally used to refer to the set of vectors joining any one of these points to all the others. (Because the points *are* a Bravais lattice, this set of vectors does not depend on which point is singled out as the origin.) Yet another usage comes from the fact that any vector  $\mathbf{R}$  determines a *translation* or *displacement*, in which everything is moved bodily through space by a distance  $R$  in the direction of  $\mathbf{R}$ . The term “Bravais lattice” is also used to refer to the set of translations determined by the vectors, rather than the vectors themselves. In practice it is always clear from the context whether it is the points, the vectors, or the translations that are being referred to.<sup>7</sup>

<sup>7</sup> The more general use of the term provides an elegant definition of a Bravais lattice with the precision of definition (b) and the nonprejudicial nature of definition (a): A Bravais lattice is a discrete set of vectors not all in a plane, closed under vector addition and subtraction (i.e., the sum and difference of any two vectors in the set are also in the set).



## COORDINATION NUMBER

The points in a Bravais lattice that are closest to a given point are called its *nearest neighbors*. Because of the periodic nature of a Bravais lattice, each point has the same number of nearest neighbors. This number is thus a property of the lattice, and is referred to as the *coordination number* of the lattice. A simple cubic lattice has coordination number 6; a body-centered cubic lattice, 8; and a face-centered cubic lattice, 12. The notion of a coordination number can be extended in the obvious way to some simple arrays of points that are not Bravais lattices, provided that each point in the array has the same number of nearest neighbors.

## PRIMITIVE UNIT CELL

A volume of space that, when translated through all the vectors in a Bravais lattice, just fills all of space without either overlapping itself or leaving voids is called a *primitive cell* or *primitive unit cell* of the lattice.<sup>8</sup> There is no unique way of choosing a primitive cell for a given Bravais lattice. Several possible choices of primitive cells for a two-dimensional Bravais lattice are illustrated in Figure 4.10.

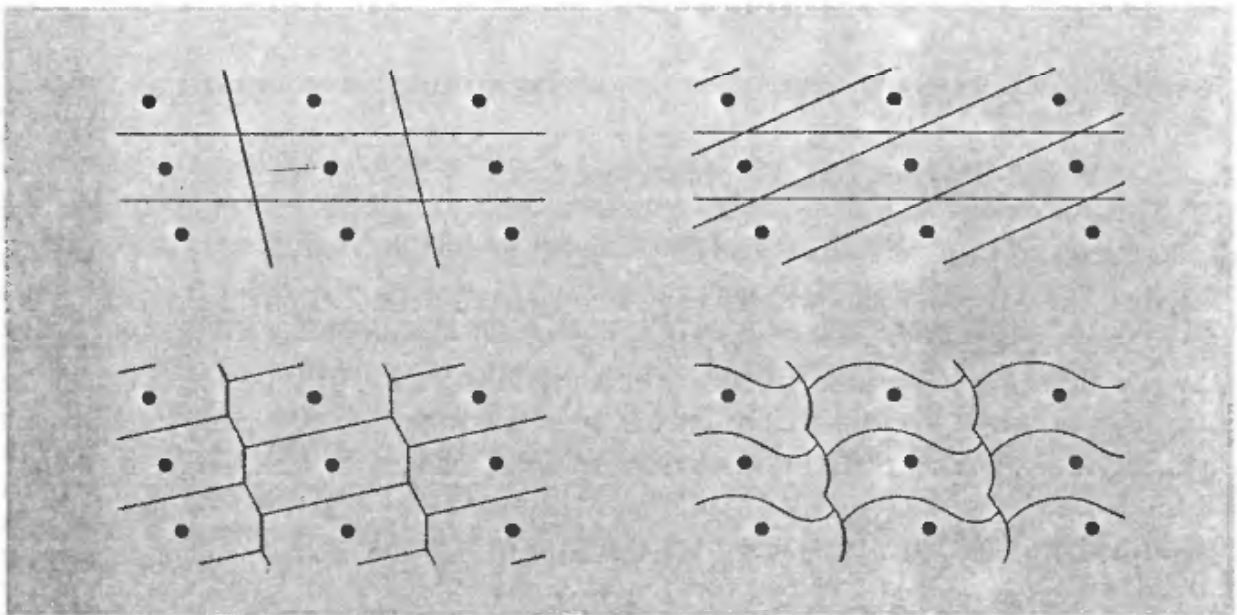


Figure 4.10

Several possible choices of primitive cell for a single two-dimensional Bravais lattice.

A primitive cell must contain precisely one lattice point (unless it is so positioned that there are points on its surface). It follows that if  $n$  is the density of points in the lattice<sup>9</sup> and  $v$  is the volume of the primitive cell, then  $nv = 1$ . Thus  $v = 1/n$ . Since

<sup>8</sup> Translations of the primitive cell may possess common surface points; the nonoverlapping proviso is only intended to prohibit overlapping regions of nonzero volume.

<sup>9</sup> The density  $n$  of Bravais lattice points need not, of course, be identical to the density of conduction electrons in a metal. When the possibility of confusion is present, we shall specify the two densities with different symbols.

this result holds for any primitive cell, the volume of a primitive cell is independent of the choice of cell.

It also follows from the definition of a primitive cell that, given any two primitive cells of arbitrary shape, it is possible to cut the first up into pieces, which, when translated through appropriate lattice vectors, can be reassembled to give the second. This is illustrated in Figure 4.11.

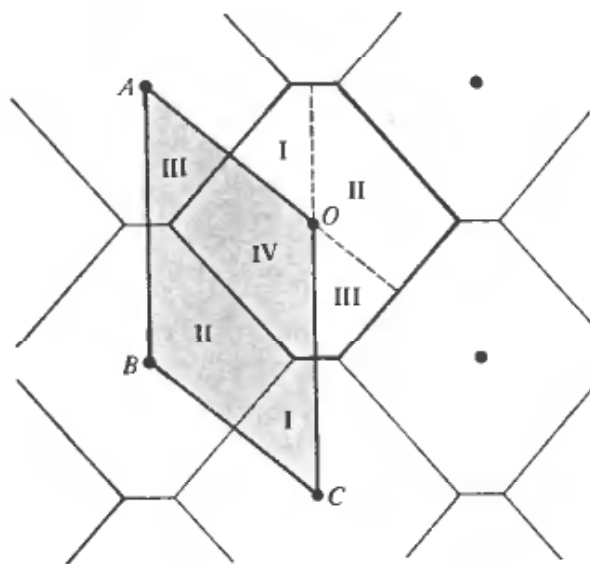


Figure 4.11

Two possible primitive cells for a two-dimensional Bravais lattice. The parallelogram cell (shaded) is obviously primitive; additional hexagonal cells are indicated to demonstrate that the hexagonal cell is also primitive. The parallelogram can be cut into pieces, which, when translated through lattice vectors, reassemble to form the hexagon. The translations for the four regions of the parallelogram are: Region I— $\vec{CO}$ ; Region II— $\vec{BO}$ ; Region III— $\vec{AO}$ ; Region IV—no translation.

The obvious primitive cell to associate with a particular set of primitive vectors,  $\mathbf{a}_1, \mathbf{a}_2, \mathbf{a}_3$ , is the set of all points  $\mathbf{r}$  of the form

$$\mathbf{r} = x_1\mathbf{a}_1 + x_2\mathbf{a}_2 + x_3\mathbf{a}_3 \quad (4.6)$$

for all  $x_i$  ranging continuously between 0 and 1; i.e., the parallelepiped spanned by the three vectors  $\mathbf{a}_1, \mathbf{a}_2$ , and  $\mathbf{a}_3$ . This choice has the disadvantage of not displaying the full symmetry of the Bravais lattice. For example (Figure 4.12), the unit cell (4.6) for the choice of primitive vectors (4.5) of the fcc Bravais lattice is an oblique parallelepiped, which does not have the full cubic symmetry of the lattice in which it is embedded. It is often important to work with cells that do have the full symmetry of their Bravais lattice. There are two widely used solutions to this problem:

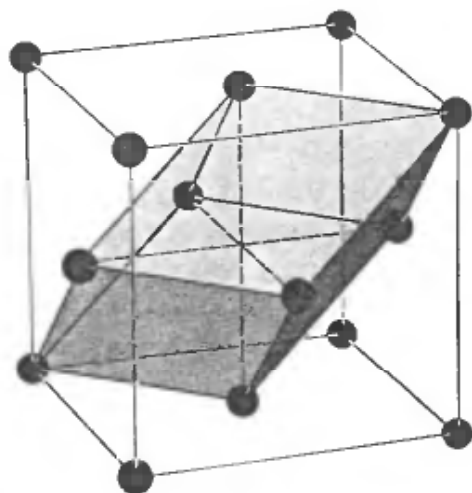


Figure 4.12

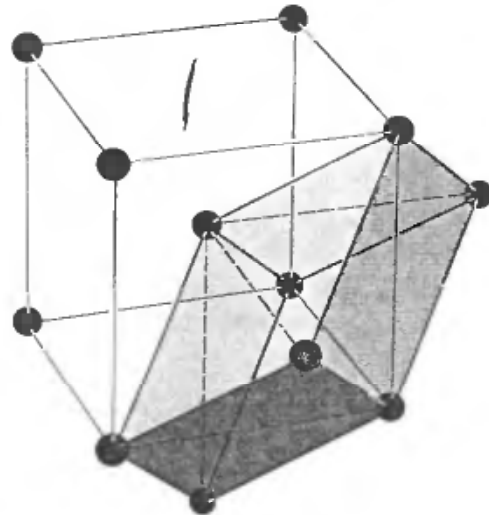
Primitive and conventional unit cells for the face-centered cubic Bravais lattice. The conventional cell is the large cube. The primitive cell is the figure with six parallelogram faces. It has one quarter the volume of the cube, and rather less symmetry.

## UNIT CELL; CONVENTIONAL UNIT CELL

One can fill space up with nonprimitive unit cells (known simply as *unit cells* or *conventional unit cells*). A unit cell is a region that just fills space without any overlapping when translated through some *subset* of the vectors of a Bravais lattice. The conventional unit cell is generally chosen to be bigger than the primitive cell and to have the required symmetry. Thus one frequently describes the body-centered cubic lattice in terms of a cubic unit cell (Figure 4.13) that is twice as large as a primitive bcc unit cell, and the face-centered cubic lattice in terms of a cubic unit cell (Figure 4.12) that has four times the volume of a primitive fcc unit cell. (That the conventional cells are two and four times bigger than the primitive cells is easily seen by asking how many lattice points the conventional cubic cell must contain when it is so placed that no points are on its surface.) Numbers specifying the size of a unit cell (such as the single number  $a$  in cubic crystals) are called *lattice constants*.

Figure 4.13

Primitive and conventional unit cells for the body-centered cubic Bravais lattice. The primitive cell (shaded) has half the volume of the conventional cubic cell.



## WIGNER-SEITZ PRIMITIVE CELL

One can always choose a *primitive* cell with the full symmetry of the Bravais lattice. By far the most common such choice is the *Wigner-Seitz cell*. The Wigner-Seitz cell about a lattice point is the region of space that is closer to that point than to any other lattice point.<sup>10</sup> Because of the translational symmetry of the Bravais lattice, the Wigner-Seitz cell about any one lattice point must be taken into the Wigner-Seitz cell about any other, when translated through the lattice vector that joins the two points. Since any point in space has a unique lattice point, as its nearest neighbor<sup>11</sup> it will belong to the Wigner-Seitz cell of precisely one lattice point. It follows that a

<sup>10</sup> Such a cell can be defined for any set of discrete points that do not necessarily form a Bravais lattice. In this broader context the cell is known as a Voronoy polyhedron. In contrast to the Wigner-Seitz cell, the structure and orientation of a general Voronoy polyhedron will depend on which point of the array it encloses.

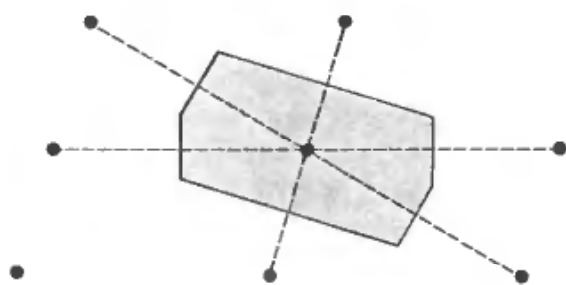
<sup>11</sup> Except for points on the common surface of two or more Wigner-Seitz cells.

Wigner-Seitz cell, when translated through all lattice vectors, will just fill space without overlapping; i.e., the Wigner-Seitz cell is a primitive cell.

Since there is nothing in the definition of the Wigner-Seitz cell that refers to any particular choice of primitive vectors, the Wigner-Seitz cell will be as symmetrical as the Bravais lattice.<sup>12</sup>

The Wigner-Seitz unit cell is illustrated for a two-dimensional Bravais lattice in Figure 4.14 and for the three-dimensional body-centered cubic and face-centered cubic Bravais lattices in Figures 4.15 and 4.16.

Note that the Wigner-Seitz unit cell about a lattice point can be constructed by drawing lines connecting the point to all others<sup>13</sup> in the lattice, bisecting each line



• **Figure 4.14**

The Wigner-Seitz cell for a two-dimensional Bravais lattice. The six sides of the cell bisect the lines joining the central points to its six nearest neighboring points (shown as dashed lines). In two dimensions the Wigner-Seitz cell is always a hexagon unless the lattice is rectangular (see Problem 4a).

**Figure 4.15**

The Wigner-Seitz cell for the body-centered cubic Bravais lattice (a “truncated octahedron”). The surrounding cube is a conventional body-centered cubic cell with a lattice point at its center and on each vertex. The hexagonal faces bisect the lines joining the central point to the points on the vertices (drawn as solid lines). The square faces bisect the lines joining the central point to the central points in each of the six neighboring cubic cells (not drawn). The hexagons are regular (see Problem 4d).

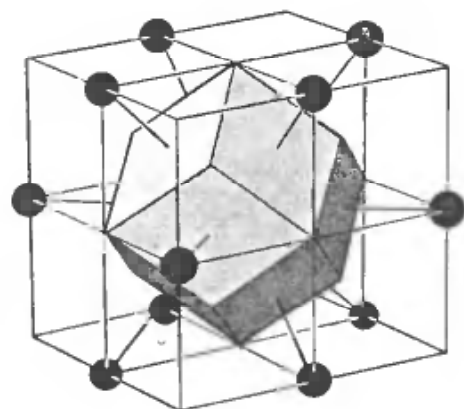
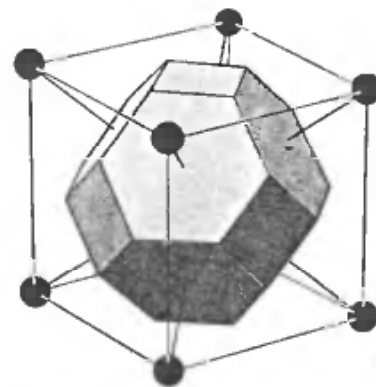


**Figure 4.16**

Wigner-Seitz cell for the face-centered cubic Bravais lattice (a “rhombic dodecahedron”). The surrounding cube is *not* the conventional cubic cell of Figure 4.12, but one in which lattice points are at the center of the cube and at the center of the 12 edges. Each of the 12 (congruent) faces is perpendicular to a line joining the central point to a point on the center of an edge.

<sup>12</sup> A precise definition of “as symmetrical as” is given in Chapter 7.

<sup>13</sup> In practice only a fairly small number of nearby points actually y<sup>i</sup> planes that bound the cell.

with a plane, and taking the smallest polyhedron containing the point bounded by these planes.

## CRYSTAL STRUCTURE; LATTICE WITH A BASIS

A physical crystal can be described by giving its underlying Bravais lattice, together with a description of the arrangement of atoms, molecules, ions, etc., within a particular primitive cell. When emphasizing the difference between the abstract pattern of points composing the Bravais lattice and an actual physical crystal<sup>14</sup> embodying the lattice, the technical term "crystal structure" is used. A *crystal structure* consists of identical copies of the same physical unit, called the *basis*, located at all the points of a Bravais lattice (or, equivalently, translated through all the vectors of a Bravais lattice). Sometimes the term *lattice with a basis* is used instead. However, "lattice with a basis" is also used in a more general sense to refer to what results even when the basic unit is *not* a physical object or objects, but another set of points. For example, the vertices of a two-dimensional honeycomb, though not a Bravais lattice, can be represented as a two-dimensional triangular Bravais lattice<sup>15</sup> with a two-point basis (Figure 4.17). A crystal structure with a basis consisting of a single atom or ion is often called a monatomic Bravais lattice.

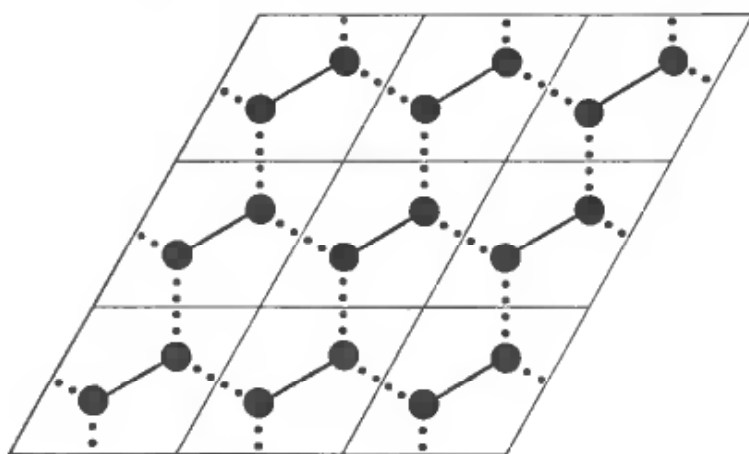


Figure 4.17

The honeycomb net, drawn so as to emphasize that it is a Bravais lattice with a two-point basis. The pairs of points joined by heavy solid lines are identically placed in the primitive cells (parallelograms) of the underlying Bravais lattice.

One also can describe a Bravais lattice as a lattice with a basis by choosing a non-primitive conventional unit cell. This is often done to emphasize the cubic symmetry of the bcc and fcc Bravais lattices, which are then described respectively, as simple cubic lattices spanned by  $a\hat{x}$ ,  $a\hat{y}$ , and  $a\hat{z}$ , with a two-point basis

$$0, \frac{a}{2}(\hat{x} + \hat{y} + \hat{z}) \quad (\text{bcc}) \quad (4.7)$$

or a four-point basis

$$0, \frac{a}{2}(\hat{x} + \hat{y}), \frac{a}{2}(\hat{y} + \hat{z}), \frac{a}{2}(\hat{z} + \hat{x}) \quad (\text{fcc}). \quad (4.8)$$

<sup>14</sup> But still idealized in being infinite in extent.

<sup>15</sup> Spanned by two primitive vectors of equal length, making an angle of  $60^\circ$ .

## SOME IMPORTANT EXAMPLES OF CRYSTAL STRUCTURES AND LATTICES WITH BASES

### Diamond Structure

The diamond lattice<sup>16</sup> (formed by the carbon atoms in a diamond crystal) consists of two interpenetrating face-centered cubic Bravais lattices, displaced along the body diagonal of the cubic cell by one quarter the length of the diagonal. It can be regarded as a face-centered cubic lattice with the two-point basis  $\mathbf{0}$  and  $(a/4)(\hat{x} + \hat{y} + \hat{z})$ . The coordination number is 4 (Figure 4.18). The diamond lattice is not a Bravais lattice,

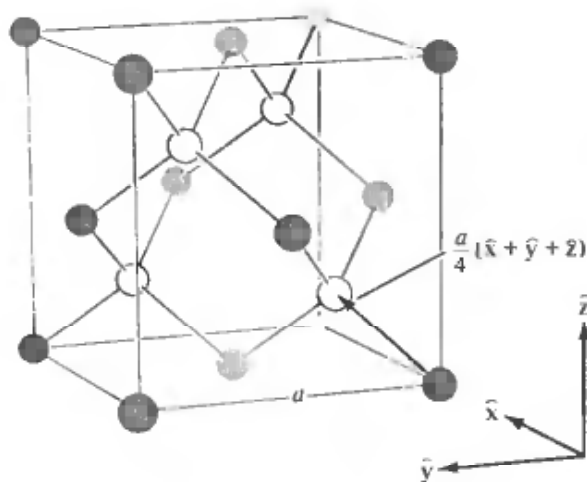


**Figure 4.18**

Conventional cubic cell of the diamond lattice. For clarity, sites corresponding to one of the two interpenetrating face-centered cubic lattices are unshaded. (In the zincblende structure the shaded sites are occupied by one kind of ion, and the unshaded by another.) Nearest-neighbor bonds have been drawn in. The four nearest neighbors of each point form the vertices of a regular tetrahedron.

because the environment of any point differs in orientation from the environments of its nearest neighbors. Elements crystallizing in the diamond structure are given in Table 4.3.

Table 4.3  
ELEMENTS WITH THE DIAMOND CRYSTAL  
STRUCTURE

ELEMENT	CUBE SIDE $a$ (Å)
C (diamond)	3.57
Si	5.43
Ge	5.66
$\alpha$ -Sn (grey)	6.49

### Hexagonal Close-Packed Structure

Though not a Bravais lattice, the *hexagonal close-packed* (hcp) structure ranks in importance with the body-centered cubic and face-centered cubic Bravais lattices; about 30 elements crystallize in the hexagonal close-packed form (Table 4.4).

<sup>16</sup> We use the word "lattice," without qualifications, to refer either to a Bravais lattice or a lattice with a basis.

Table 4.4  
ELEMENTS WITH THE HEXAGONAL CLOSE-PACKED CRYSTAL  
STRUCTURE

ELEMENT	$a$ (Å)	$c$	$c/a$	ELEMENT	$a$ (Å)	$c$	$c/a$
Be	2.29	3.58	1.56	Os	2.74	4.32	1.58
Cd	2.98	5.62	1.89	Pr	3.67	5.92	1.61
Ce	3.65	5.96	1.63	Re	2.76	4.46	1.62
$\alpha$ -Co	2.51	4.07	1.62	Ru	2.70	4.28	1.59
Dy	3.59	5.65	1.57	Sc	3.31	5.27	1.59
Er	3.56	5.59	1.57	Tb	3.60	5.69	1.58
Gd	3.64	5.78	1.59	Ti	2.95	4.69	1.59
He (2 K)	3.57	5.83	1.63	Tl	3.46	5.53	1.60
Hf	3.20	5.06	1.58	Tm	3.54	5.55	1.57
Ho	3.58	5.62	1.57	Y	3.65	5.73	1.57
La	3.75	6.07	1.62	Zn	2.66	4.95	1.86
Lu	3.50	5.55	1.59	Zr	3.23	5.15	1.59
Mg	3.21	5.21	1.62				
Nd	3.66	5.90	1.61	"Ideal"			1.63

Underlying the hcp structure is a *simple hexagonal* Bravais lattice, given by stacking two-dimensional triangular nets<sup>15</sup> directly above each other (Figure 4.19). The direction of stacking ( $\mathbf{a}_3$ , below) is known as the  $c$ -axis. Three primitive vectors are

$$\mathbf{a}_1 = a\hat{x}, \quad \mathbf{a}_2 = \frac{a}{2}\hat{x} + \frac{\sqrt{3}a}{2}\hat{y}, \quad \mathbf{a}_3 = c\hat{z}. \quad (4.9)$$

The first two generate a triangular lattice in the  $x$ - $y$  plane, and the third stacks the planes a distance  $c$  above one another.

The hexagonal close-packed structure consists of two interpenetrating simple hexagonal Bravais lattices, displaced from one another by  $\mathbf{a}_1/3 + \mathbf{a}_2/3 + \mathbf{a}_3/2$  (Figure 4.20). The name reflects the fact that close-packed hard spheres can be arranged in

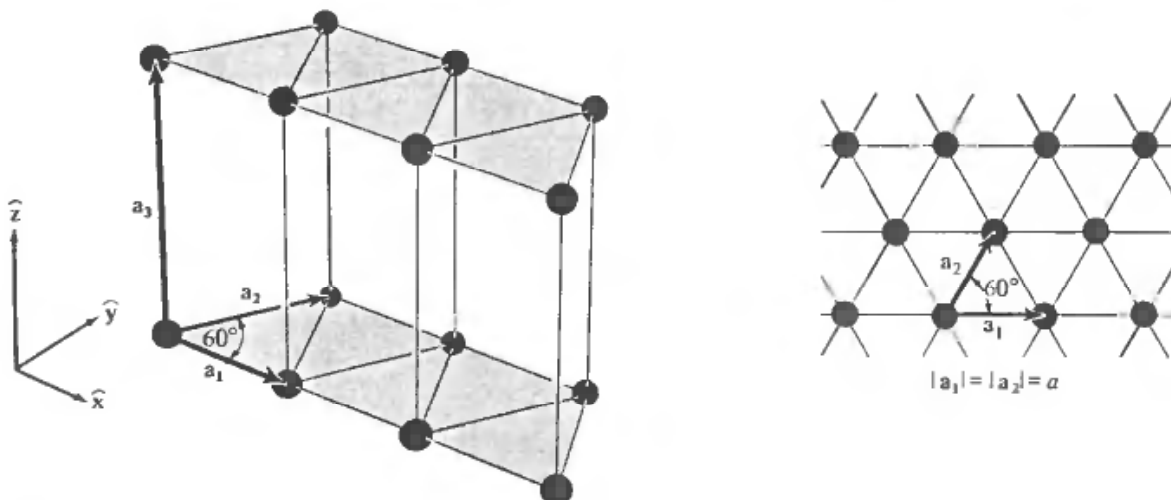


Figure 4.19  
The simple hexagonal Bravais lattice. Two-dimensional triangular nets (shown in inset) are stacked directly above one another, a distance  $c$  apart.

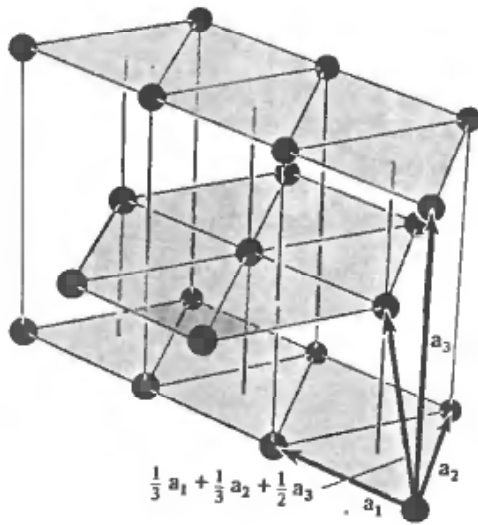


Figure 4.20

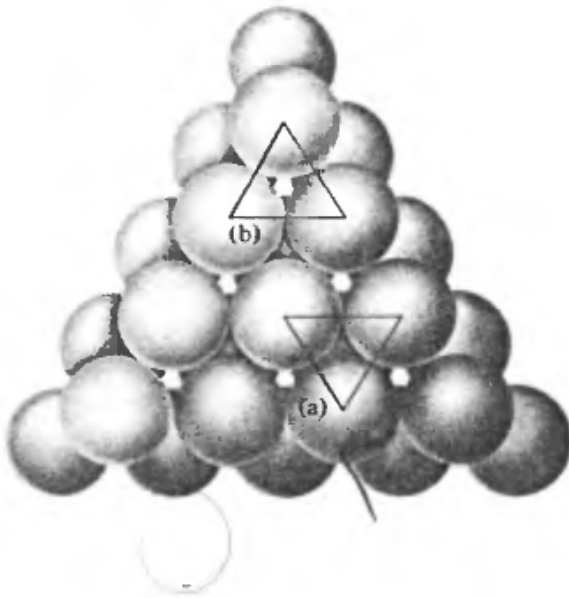
The hexagonal close-packed crystal structure. It can be viewed as two interpenetrating simple hexagonal Bravais lattices, displaced vertically by a distance  $c/2$  along the common  $c$ -axis, and displaced horizontally so that the points of one lie directly above the centers of the triangles formed by the points of the other.

such a structure. Consider stacking cannonballs (Figure 4.21), starting with a close-packed triangular lattice as the first layer. The next layer is formed by placing a ball in the depressions left in the center of every other triangle in the first layer, thereby forming a second triangular layer, shifted with respect to the first. The third layer is formed by placing balls in alternate depressions in the second layer, so that they lie directly over the balls in the first layer. The fourth layer lies directly over the second, and so on. The resulting lattice is hexagonal close-packed with the particular value (see Problem 5):

$$c = \sqrt{\frac{8}{3}} a = 1.63299a. \quad (4.10)$$

Figure 4.21

View from above of the first two layers in a stack of cannonballs. The first layer is arranged in a plane triangular lattice. Balls in the second layer are placed above alternate interstices in the first. If balls in the third layer are placed directly above those in the first, at sites of the type shown in inset (a), balls in the fourth directly above those in the second, etc., the resulting structure will be close-packed hexagonal. If, however, balls in the third layer are placed directly above those interstices in the first that were *not* covered by balls in the second, at sites of the type shown in inset (b), balls in the fourth layer placed directly above those in the first, balls in the fifth directly above those in the second, etc., the resulting structure will be face-centered cubic (with the body diagonal of the cube oriented vertically.)



Because, however, the symmetry of the hexagonal close-packed lattice is independent of the  $c/a$  ratio, the name is not restricted to this case. The value  $c/a = \sqrt{8/3}$  is sometimes called “ideal,” and the truly close-packed structure, with the ideal value of  $c/a$ , is known as an ideal hcp structure. Unless, however, the physical units in the hcp structure are actually close-packed spheres, there is no reason why  $c/a$  should be ideal (see Table 4.4).



Note, as in the case of the diamond structure, that the hcp lattice is not a Bravais lattice, because the orientation of the environment of a point varies from layer to layer along the  $c$ -axis. Note also that, when viewed along the  $c$ -axis, the two types of planes merge to form the two-dimensional honeycomb array of Figure 4.3, which is not a Bravais lattice.

### Other Close-Packing Possibilities

Note that the hcp structure is not the only way to close-pack spheres. If the first two layers are laid down as described above, but the third is placed in the *other* set of depressions in the second—i.e., those lying above unused depressions in *both* the first and second layers (see Figure 4.21)—and then the fourth layer is placed in depressions in the third directly above the balls in the first, the fifth above the second, and so on, one generates a Bravais lattice. This Bravais lattice turns out to be nothing but the face-centered cubic lattice, with the cube diagonal perpendicular to the triangular planes (Figures 4.22 and 4.23).

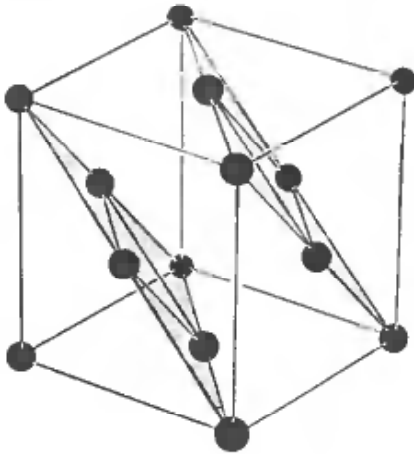
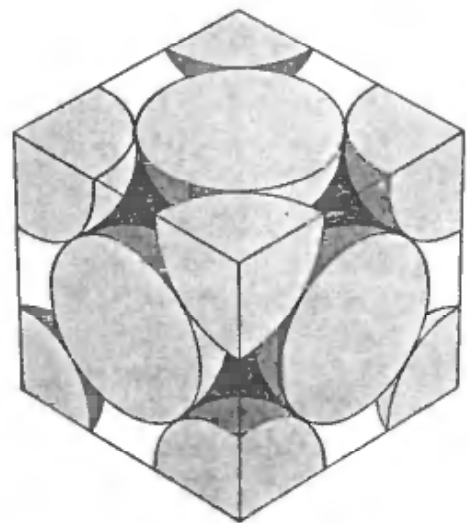


Figure 4.22  
How to section the face-centered cubic Bravais lattice to get the layers pictured in Figure 4.21.

Figure 4.23  
A cubic section of some face-centered cubic close-packed spheres.



There are infinitely many other close-packing arrangements, since each successive layer can be placed in either of two positions. Only fcc close-packing gives a Bravais lattice, and the fcc (...*ABCABCABC*...) and hcp (...*ABABAB*...) structures are by far the most commonly encountered. Other close-packed structures are observed, however. Certain rare earth metals, for example, take on a structure of the form (...*ABACABACABAC*...).

### The Sodium Chloride Structure

We are forced to describe the hexagonal close-packed and diamond lattices as lattices with bases by the intrinsic geometrical arrangement of the lattice points. A lattice with a basis is also necessary, however, in describing crystal structures in which the atoms or ions are located only at the points of a Bravais lattice, but in which the crystal structure nevertheless lacks the full translational symmetry of the Bravais lattice because more than one kind of atom or ion is present. For example, sodium chloride (Figure 4.24) consists of equal numbers of sodium and chlorine ions placed at alternate points of a simple cubic lattice, in such a way that each ion has six of the other kind of ions as its nearest neighbors.<sup>17</sup> This structure can be described as a face-centered cubic Bravais lattice with a basis consisting of a sodium ion at  $\mathbf{0}$  and a chlorine ion at the center of the conventional cubic cell,  $(a/2)(\hat{x} + \hat{y} + \hat{z})$ .

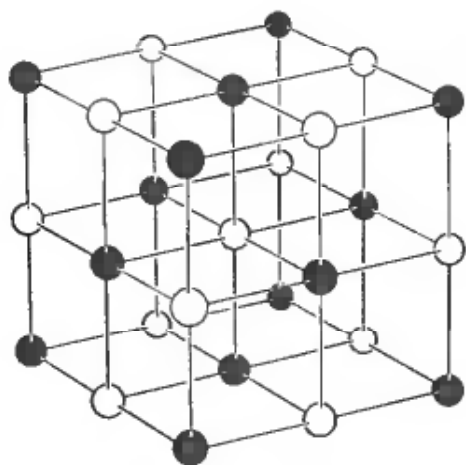


Figure 4.24

The sodium chloride structure. One type of ion is represented by black balls, the other type by white. The black and white balls form interpenetrating fcc lattices.

Table 4.5

SOME COMPOUNDS WITH THE SODIUM CHLORIDE STRUCTURE

CRYSTAL	$a$ (Å)	CRYSTAL	$a$ (Å)	CRYSTAL	$a$ (Å)
LiF	4.02	RbF	5.64	CaS	5.69
LiCl	5.13	RbCl	6.58	CaSe	5.91
LiBr	5.50	RbBr	6.85	CaTe	6.34
LiI	6.00	RbI	7.34	SrO	5.16
NaF	4.62	CsF	6.01	SrS	6.02
NaCl	5.64	AgF	4.92	SrSe	6.23
NaBr	5.97	AgCl	5.55	SrTe	6.47
NaI	6.47	AgBr	5.77	BaO	5.52
KF	5.35	MgO	4.21	BaS	6.39
KCl	6.29	MgS	5.20	BaSe	6.60
KBr	6.60	MgSe	5.45	BaTe	6.99
KI	7.07	CaO	4.81		

### The Cesium Chloride Structure

Similarly, cesium chloride (Figure 4.25) consists of equal numbers of cesium and chlorine ions, placed at the points of a body-centered cubic lattice so that each ion

<sup>17</sup> For examples see Table 4.5.

has eight of the other kind as its nearest neighbors.<sup>18</sup> The translational symmetry of this structure is that of the simple cubic Bravais lattice, and it is described as a simple cubic lattice with a basis consisting of a cesium ion at the origin  $0$  and a chlorine ion at the cube center  $(a/2)(\hat{x} + \hat{y} + \hat{z})$ .

Figure 4.25

The cesium chloride structure. One type of ion is represented by black balls, the other type by white. The black and white balls form interpenetrating simple cubic lattices.

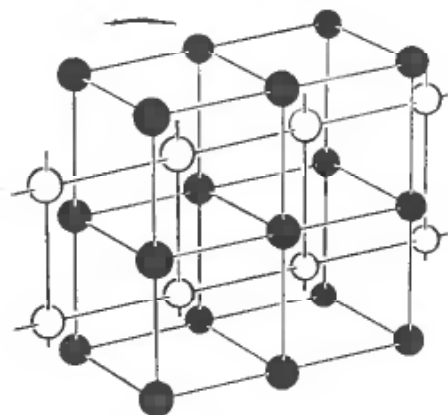


Table 4.6  
SOME COMPOUNDS WITH THE CESIUM CHLORIDE  
STRUCTURE

CRYSTAL	$a$ (Å)	CRYSTAL	$a$ (Å)
CsCl	4.12	TlCl	3.83
CsBr	4.29	TlBr	3.97
CsI	4.57	TlI	4.20

### The Zincblende Structure

Zincblende has equal numbers of zinc and sulfur ions distributed on a diamond lattice so that each has four of the opposite kind as nearest neighbors (Figure 4.18). This structure<sup>19</sup> is an example of a lattice with a basis, which must be so described both because of the geometrical position of the ions and because two types of ions occur.

Table 4.7  
SOME COMPOUNDS WITH THE ZINCBLLENDE STRUCTURE

CRYSTAL	$a$ (Å)	CRYSTAL	$a$ (Å)	CRYSTAL	$a$ (Å)
CuF	4.26	ZnS	5.41	AlSb	6.13
CuCl	5.41	ZnSe	5.67	GaP	5.45
CuBr	5.69	ZnTe	6.09	GaAs	5.65
CuI	6.04	CdS	5.82	GaSb	6.12
AgI	6.47	CdTe	6.48	InP	5.87
BeS	4.85	HgS	5.85	InAs	6.04
BeSe	5.07	HgSe	6.08	InSb	6.48
BeTe	5.54	HgTe	6.43	SiC	4.35
MnS (red)	5.60	AlP	5.45		
MnSe	5.82	AlAs	5.62		

<sup>18</sup> For examples see Table 4.6.

<sup>19</sup> For example see Table 4.7.

## OTHER ASPECTS OF CRYSTAL LATTICES

This chapter has concentrated on the description of the *translational* symmetry of crystal lattices in *real physical space*. Two other aspects of periodic arrays will be dealt with in subsequent chapters: in Chapter 5 we examine the consequences of translational symmetry not in real space, but in the so-called *reciprocal* (or *wave vector*) *space*, and in Chapter 7 we describe some features of the *rotational* symmetry of crystal lattices.

## PROBLEMS

- In each of the following cases indicate whether the structure is a Bravais lattice. If it is, give three primitive vectors; if it is not, describe it as a Bravais lattice with as small as possible a basis.
  - Base-centered cubic (simple cubic with additional points in the centers of the horizontal faces of the cubic cell).
  - Side-centered cubic (simple cubic with additional points in the centers of the vertical faces of the cubic cell).
  - Edge-centered cubic (simple cubic with additional points at the midpoints of the lines joining nearest neighbors).
- What is the Bravais lattice formed by all points with Cartesian coordinates  $(n_1, n_2, n_3)$  if:
  - The  $n_i$  are either all even or all odd?
  - The sum of the  $n_i$  is required to be even?
- Show that the angle between any two of the lines (bonds) joining a site of the diamond lattice to its four nearest neighbors is  $\cos^{-1}(-1/3) = 109^\circ 28'$ .
- Prove that the Wigner-Seitz cell for any two-dimensional Bravais lattice is either a hexagon or a rectangle.
  - Show that the ratio of the lengths of the diagonals of each parallelogram face of the Wigner-Seitz cell for the face-centered cubic lattice (Figure 4.16) is  $\sqrt{2}:1$ .
  - Show that every edge of the polyhedron bounding the Wigner-Seitz cell of the body-centered cubic lattice (Figure 4.15) is  $\sqrt{2}/4$  times the length of the conventional cubic cell.
  - Prove that the hexagonal faces of the bcc Wigner-Seitz cell are all regular hexagons. (Note that the axis perpendicular to a hexagonal face passing through its center has only threefold symmetry, so this symmetry alone is not enough.)
- Prove that the ideal  $c/a$  ratio for the hexagonal close-packed structure is  $\sqrt{8/3} = 1.633$ .
  - Sodium transforms from bcc to hcp at about 23K (the "martensitic" transformation). Assuming that the density remains fixed through this transition, find the lattice constant  $a$  of the hexagonal phase, given that  $a = 4.23 \text{ \AA}$  in the cubic phase and that the  $c/a$  ratio is indistinguishable from its ideal value.
- The face-centered cubic is the most dense and the simple cubic is the least dense of the three cubic Bravais lattices. The diamond structure is less dense than any of these. One measure of this is that the coordination numbers are: fcc, 12; bcc, 8; sc, 6; diamond, 4. Another is the following: Suppose identical solid spheres are distributed through space in such a way that their centers

# 27

## *Dielectric Properties of Insulators*

Macroscopic Electrostatic Maxwell Equations

Theory of the Local Field

Clausius-Mossotti Relation

Theory of the Polarizability

Long-Wavelength Optical Modes in Ionic Crystals

Optical Properties of Ionic Crystals

Reststrahlen

Covalent Insulators

Pyroelectric and Ferroelectric Crystals

Because charge cannot flow freely in insulators, applied electric fields of substantial amplitude can penetrate into their interiors. There are at least three broad contexts in which it is important to know how the internal structure of an insulator, both electronic and ionic, readjusts when an additional electric field is superimposed on the electric field associated with the periodic lattice potential:

1. We may place a sample of the insulator in a static electric field such as that existing between the plates of a capacitor. Many important consequences of the resulting internal distortion can be deduced if one knows the static dielectric constant  $\epsilon_0$  of the crystal, whose calculation is therefore an important aim of any microscopic theory of insulators.
2. We may be interested in the optical properties of the insulator—i.e., in its response to the AC electric field associated with electromagnetic radiation. In this case the important quantity to calculate is the frequency-dependent dielectric constant  $\epsilon(\omega)$ , or, equivalently, the index of refraction,  $n = \sqrt{\epsilon}$ .
3. In an ionic crystal, even in the absence of externally applied fields, there may be long-range electrostatic forces between the ions in addition to the periodic lattice potential, when the lattice is deformed from its equilibrium configuration (as, for example, in the course of executing a normal mode). Such forces are often best dealt with by considering the additional electric field giving rise to them, whose sources are intrinsic to the crystal.

In dealing with any of these phenomena the theory of the macroscopic Maxwell equations in a medium is a most valuable tool. We begin with a review of the electrostatic aspects of this theory.

## MACROSCOPIC MAXWELL EQUATIONS OF ELECTROSTATICS

When viewed on the atomic scale, the charge density  $\rho^{\text{micro}}(\mathbf{r})$  of any insulator is a very rapidly varying function of position, reflecting the microscopic atomic structure of the insulator. On the same atomic scale the electrostatic potential  $\phi^{\text{micro}}(\mathbf{r})$  and the electric field  $\mathbf{E}^{\text{micro}}(\mathbf{r}) = -\nabla\phi^{\text{micro}}(\mathbf{r})$  also have strong and rapid variations since they are related to  $\rho^{\text{micro}}(\mathbf{r})$  by

$$\nabla \cdot \mathbf{E}^{\text{micro}}(\mathbf{r}) = 4\pi\rho^{\text{micro}}(\mathbf{r}). \quad (27.1)$$

On the other hand, in the conventional *macroscopic* electromagnetic theory of an insulator the charge density  $\rho(\mathbf{r})$ , potential  $\phi(\mathbf{r})$ , and electric field  $\mathbf{E}(\mathbf{r})$  show no such rapid variation.<sup>1</sup> Specifically, in the case of an insulator bearing no excess charge beyond that of its component ions (or atoms or molecules), the macroscopic electrostatic field is determined by the macroscopic Maxwell equation:<sup>2</sup>

$$\nabla \cdot \mathbf{D}(\mathbf{r}) = 0, \quad (27.2)$$

<sup>1</sup> Indeed, in an insulating medium in the absence of any externally applied fields,  $\phi(\mathbf{r})$  is zero (or constant).

<sup>2</sup> More generally, one writes  $\nabla \cdot \mathbf{D} = 4\pi\rho$ , where  $\rho$  is the so-called free charge—i.e., that part of the macroscopic charge density due to excess charges not intrinsic to the medium. Throughout the following discussion we assume that there is no free charge, so that our macroscopic charge density is always the so-called bound charge of macroscopic electrostatics. The inclusion of free charge is straightforward, but not relevant to any of the applications we wish to make here.

in conjunction with the equation giving the macroscopic electric field  $\mathbf{E}$  in terms of the electric displacement  $\mathbf{D}$  and polarization density  $\mathbf{P}$ ,

$$\mathbf{D}(\mathbf{r}) = \mathbf{E}(\mathbf{r}) + 4\pi\mathbf{P}(\mathbf{r}). \quad (27.3)$$

These imply (in the absence of free charge) that the macroscopic electric field satisfies

$$\nabla \cdot \mathbf{E}(\mathbf{r}) = -4\pi\nabla \cdot \mathbf{P}(\mathbf{r}), \quad (27.4)$$

where  $\mathbf{P}$  (to be defined in detail below) is generally a very slowly varying function of position inside an insulator.

Although it is very convenient to work with the macroscopic Maxwell equations, it is also essential to deal with the microscopic field acting on individual ions.<sup>3</sup> One must therefore keep the relation between macroscopic and microscopic quantities clearly in mind. The connection, first derived by Lorentz, can be made as follows:<sup>4</sup>

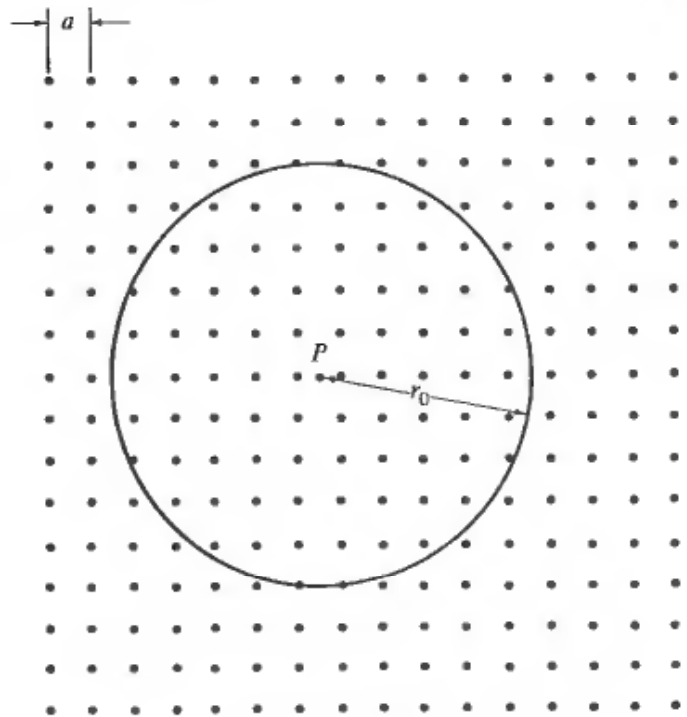
Suppose we have an insulator (not necessarily in its equilibrium configuration) that is described (at an instant) by a microscopic charge density  $\rho^{\text{micro}}(\mathbf{r})$ , which reflects the detailed atomic arrangement of electrons and nuclei and which gives rise to the rapidly varying microscopic field,  $\mathbf{E}^{\text{micro}}(\mathbf{r})$ . The macroscopic field  $\mathbf{E}(\mathbf{r})$  is defined to be an average of  $\mathbf{E}^{\text{micro}}$  over a region about  $\mathbf{r}$  that is small on the macroscopic scale, but large compared with characteristic atomic dimensions  $a$  (Figure 27.1). We make the averaging procedure explicit by using a positive normalized weight function  $f$ , satisfying:

$$f(\mathbf{r}) \geq 0; \quad f(\mathbf{r}) = 0, \quad r > r_0; \quad \int d\mathbf{r} f(\mathbf{r}) = 1; \quad f(-\mathbf{r}) = f(\mathbf{r}). \quad (27.5)$$

The distance  $r_0$  beyond which  $f$  vanishes is large compared with atomic dimensions

**Figure 27.1**

The value of a macroscopic quantity at a point  $P$  is an average of the microscopic quantity over a region of dimensions  $r_0$  in the neighborhood of  $P$ , where  $r_0$  is large compared to the interparticle spacing  $a$ .



<sup>3</sup> We continue with our convention of using the single term "ion" to refer to the ions in ionic crystals, but also the atoms or molecules making up molecular crystals.

<sup>4</sup> The following discussion is very similar to a derivation of all the macroscopic Maxwell equations by G. Russakoff, *Am. J. Phys.* **10**, 1188 (1970).

$a$ , but small on the scale over which macroscopically defined quantities vary.<sup>5</sup> We also require that  $f$  vary slowly; i.e.,  $|\nabla f|/f$  should not be appreciably greater than the minimum value, of order  $1/r_0$ , required by Eqs. (27.5). Beyond these assumptions, the form of the macroscopic theory is independent of the properties of the weight function  $f$ .

We can now give a precise definition of the macroscopic electric field  $\mathbf{E}(\mathbf{r})$  at the point  $\mathbf{r}$ : it is the average of the microscopic field in a region of radius  $r_0$  about  $\mathbf{r}$ , with points displaced by  $-\mathbf{r}'$  from  $\mathbf{r}$  receiving a weight proportional to  $f(\mathbf{r}')$ ; i.e.,

$$\mathbf{E}(\mathbf{r}) = \int d\mathbf{r}' \mathbf{E}^{\text{micro}}(\mathbf{r} - \mathbf{r}') f(\mathbf{r}'). \quad (27.6)$$

Loosely speaking, the operation specified by (27.6) washes out those features of the microscopic field that vary rapidly on the scale of  $r_0$ , and preserves those features that vary slowly on the scale of  $r_0$  (Figure 27.2). Note, for example, that if  $\mathbf{E}^{\text{micro}}$  should happen to vary slowly on the scale of  $r_0$  (as would be the case if the point  $\mathbf{r}$  were in empty space, far from the insulator), then  $\mathbf{E}(\mathbf{r})$  would equal  $\mathbf{E}^{\text{micro}}(\mathbf{r})$ .

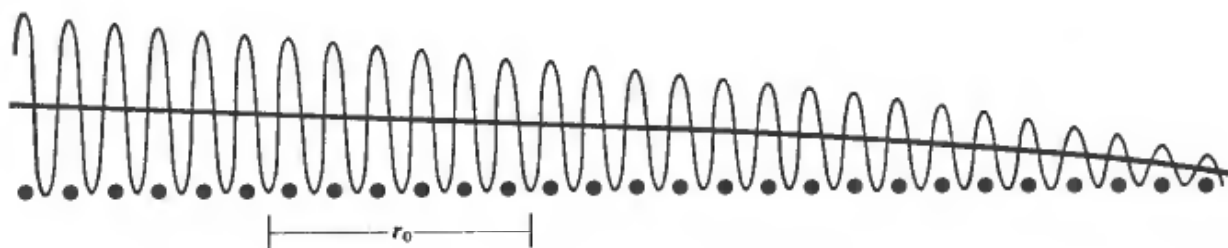


Figure 27.2

The lighter rapidly oscillatory curve illustrates the characteristic spatial variation of a microscopic quantity. The heavier curve is the corresponding macroscopic quantity. Only spatial variations that occur on a scale comparable to or larger than  $r_0$  are preserved in the macroscopic quantity.

Equations (27.6) and (27.1) immediately imply that

$$\begin{aligned} \nabla \cdot \mathbf{E}(\mathbf{r}) &= \int d\mathbf{r}' \nabla \cdot \mathbf{E}^{\text{micro}}(\mathbf{r} - \mathbf{r}') f(\mathbf{r}') \\ &= 4\pi \int d\mathbf{r}' \rho^{\text{micro}}(\mathbf{r} - \mathbf{r}') f(\mathbf{r}'). \end{aligned} \quad (27.7)$$

Therefore, to establish (27.4) we must show that

$$\int d\mathbf{r}' \rho^{\text{micro}}(\mathbf{r} - \mathbf{r}') f(\mathbf{r}') d\mathbf{r}' = -\nabla \cdot \mathbf{P}(\mathbf{r}), \quad (27.8)$$

where  $\mathbf{P}(\mathbf{r})$  is a slowly varying function that can be interpreted as a dipole moment density.

<sup>5</sup> More precisely, the macroscopic Maxwell equations are valid only when the variation in the macroscopic fields is sufficiently slow that their minimum characteristic wavelength allows a choice of  $r_0$  satisfying  $\lambda \gg r_0 \gg a$ . This condition can be satisfied by the field associated with visible light ( $\lambda \sim 10^4 a$ ), but not by the field associated with X rays ( $\lambda \sim a$ ).



We shall discuss only the case in which the microscopic charge density can be resolved into a sum of contributions from ions (or atoms or molecules) located at positions  $\mathbf{r}_j$  characterized by individual charge distributions  $\rho_j(\mathbf{r} - \mathbf{r}_j)$ :

$$\rho^{\text{micro}}(\mathbf{r}) = \sum_j \rho_j(\mathbf{r} - \mathbf{r}_j). \quad (27.9)$$

Such a resolution is quite natural in ionic or molecular solids, but is rather more difficult to achieve in covalent crystals, where important parts of the electronic charge distribution are not readily associated with a particular site in the crystal. Our discussion is therefore primarily applicable to the former two insulating categories. Quite a different approach is required to calculate the dielectric properties of covalent crystals. We shall return to this point below.

We are interested in nonequilibrium configurations of the insulator in which the ions are displaced from their equilibrium positions  $\mathbf{r}_j^0$  and are deformed from their equilibrium shapes,<sup>6</sup> which are described by charge densities  $\rho_j^0$ . Thus  $\rho^{\text{micro}}(\mathbf{r})$  will not, in general, be equal to the equilibrium microscopic charge density,

$$\rho_0^{\text{micro}}(\mathbf{r}) = \sum_j \rho_j^0(\mathbf{r} - \mathbf{r}_j^0). \quad (27.10)$$

Using (27.9) we can write (27.7) as:

$$\begin{aligned} \nabla \cdot \mathbf{E}(\mathbf{r}) &= 4\pi \sum_j \int d\mathbf{r}' \rho_j(\mathbf{r} - \mathbf{r}_j - \mathbf{r}') f(\mathbf{r}') \\ &= 4\pi \sum_j \int d\bar{\mathbf{r}} \rho_j(\bar{\mathbf{r}}) f(\mathbf{r} - \mathbf{r}_j^0 - (\bar{\mathbf{r}} + \Delta_j)), \end{aligned} \quad (27.11)$$

where  $\Delta_j = \mathbf{r}_j - \mathbf{r}_j^0$ . The displacement  $\Delta_j$  of the  $j$ th ion from its equilibrium position is a microscopic distance of order  $a$  or less. Furthermore the charge density  $\rho_j(\bar{\mathbf{r}})$  vanishes when  $\bar{\mathbf{r}}$  exceeds a microscopic distance of order  $a$ . Since the variation in the weight function  $f$  is very small over distances of order  $a$ , we can expand (27.11) in what is effectively a series in powers of  $a/r_0$  by using the Taylor expansion:

$$f(\mathbf{r} - \mathbf{r}_j^0 - (\bar{\mathbf{r}} + \Delta_j)) = \sum_{n=0}^{\infty} \frac{1}{n!} \left[ -(\bar{\mathbf{r}} + \Delta_j) \cdot \nabla \right]^n f(\mathbf{r} - \mathbf{r}_j^0). \quad (27.12)$$

If we substitute the first two terms<sup>7</sup> from (27.12) into (27.11) we find that

$$\nabla \cdot \mathbf{E}(\mathbf{r}) = 4\pi \left[ \sum_j e_j f(\mathbf{r} - \mathbf{r}_j^0) - \sum_j (\mathbf{p}_j + e_j \Delta_j) \cdot \nabla f(\mathbf{r} - \mathbf{r}_j^0) \right], \quad (27.13)$$

where

$$e_j = \int d\bar{\mathbf{r}} \rho_j(\bar{\mathbf{r}}), \quad \mathbf{p}_j = \int d\bar{\mathbf{r}} \rho_j(\bar{\mathbf{r}}) \bar{\mathbf{r}}. \quad (27.14)$$

<sup>6</sup> We have in mind applications (a) to monatomic Bravais lattices (in which the  $\mathbf{r}_j^0$  are just the Bravais lattice vectors  $\mathbf{R}$  and all of the functions  $\rho_j^0$  are identical, and (b) to lattices with a basis, in which the  $\mathbf{r}_j^0$  run through all vectors  $\mathbf{R}, \mathbf{R} + \mathbf{d}$ , etc., and there are as many distinct functional forms for the  $\rho_j^0$  as there are distinct types of ions in the basis.

<sup>7</sup> We shall find that the first ( $n = 0$ ) term makes no contribution to (27.11), and we must therefore retain the next ( $n = 1$ ) term to get the leading contribution.

The quantities  $e_j$  and  $\mathbf{p}_j$  are simply the total charge and dipole moment of the  $j$ th ion.

In the case of a monatomic Bravais lattice the charge of each "ion" must be zero (since the crystal is neutral and all "ions" are identical). In addition the equilibrium positions  $\mathbf{r}_j^0$  are the Bravais lattice sites  $\mathbf{R}$ , so (27.13) reduces to

$$\nabla \cdot \mathbf{E}(\mathbf{r}) = -4\pi \nabla \cdot \sum_{\mathbf{R}} f(\mathbf{r} - \mathbf{R})\mathbf{p}(\mathbf{R}), \quad (27.15)$$

where  $\mathbf{p}(\mathbf{R})$  is the dipole moment of the atom at site  $\mathbf{R}$ .

With a straightforward generalization of the definition of  $\mathbf{p}(\mathbf{R})$ , this result remains valid (to leading order in  $a/r_0$ ) even when we allow for ionic charge and a polyatomic basis. To see this, suppose that the  $\mathbf{r}_j^0$  now run through the sites  $\mathbf{R} + \mathbf{d}$  of a lattice with a basis. We can then label  $p_j$  and  $e_j$  by the Bravais lattice vector  $\mathbf{R}$  and basis vector  $\mathbf{d}$  specifying the equilibrium position of the  $j$ th ion:<sup>8</sup>

$$\mathbf{p}_j \rightarrow \mathbf{p}(\mathbf{R}, \mathbf{d}), \quad e_j \rightarrow e(\mathbf{d}), \quad \mathbf{r}_j^0 \rightarrow \mathbf{R} + \mathbf{d}, \quad \Delta_j \rightarrow \mathbf{u}(\mathbf{R}, \mathbf{d}). \quad (27.16)$$

Since  $d$  is a microscopic length of order  $a$ , we can perform the further expansion:

$$f(\mathbf{r} - \mathbf{R} - \mathbf{d}) \approx f(\mathbf{r} - \mathbf{R}) - \mathbf{d} \cdot \nabla f(\mathbf{r} - \mathbf{R}). \quad (27.17)$$

Substituting this into (27.13) and dropping terms of higher than linear order in  $a/r_0$ , we again recover (27.15), where  $\mathbf{p}(\mathbf{R})$  is now the dipole moment of the entire primitive cell<sup>9</sup> associated with  $\mathbf{R}$ :

$$\mathbf{p}(\mathbf{R}) = \sum_{\mathbf{d}} [e(\mathbf{d})\mathbf{u}(\mathbf{R}, \mathbf{d}) + \mathbf{p}(\mathbf{R}, \mathbf{d})]. \quad (27.18)$$

Comparing (27.15) with the macroscopic Maxwell equation (27.4), we find that the two are consistent if the polarization density is defined by

$$\mathbf{P}(\mathbf{r}) = \sum_{\mathbf{R}} f(\mathbf{r} - \mathbf{R})\mathbf{p}(\mathbf{R}). \quad (27.19)$$

If we are dealing with distortions from equilibrium whose form does not vary much from cell to cell on the microscopic scale, then  $\mathbf{p}(\mathbf{R})$  will vary only slowly from cell to cell, and we can evaluate (27.19) as an integral:

$$\mathbf{P}(\mathbf{r}) = \frac{1}{v} \sum_{\mathbf{R}} v f(\mathbf{r} - \mathbf{R})\mathbf{p}(\mathbf{R}) \approx \frac{1}{v} \int d\bar{\mathbf{r}} f(\mathbf{r} - \bar{\mathbf{r}})\mathbf{p}(\bar{\mathbf{r}}), \quad (27.20)$$

where  $\mathbf{p}(\bar{\mathbf{r}})$  is a smooth, slowly varying continuous function equal to the polarization of the cells in the immediate vicinity of  $\bar{\mathbf{r}}$ , and  $v$  is the volume of the equilibrium primitive cell.

<sup>8</sup> Ions separated by Bravais lattice vectors have the same total charge, so  $e_j$  depends only on  $\mathbf{d}$ , and not on  $\mathbf{R}$ .

<sup>9</sup> In deriving (27.18) we have used the fact that the total charge of the primitive cell,  $\sum e(\mathbf{d})$ , vanishes. We have also neglected an additional term,  $\sum d e(\mathbf{d})$ , which is the dipole moment of the primitive cell in the undistorted equilibrium crystal. In most crystals this term vanishes for the most natural choices of primitive cell. If it did not vanish, the crystal would have a polarization density in equilibrium in the absence of distorting forces or external electric fields. Such crystals do exist, and are known as pyroelectrics. We shall discuss them later in this chapter, where we shall also make clearer what is meant by "most natural choices of primitive cell" (see page 554).

We shall restrict our use of the macroscopic Maxwell equations to situations in which the variation in cellular polarization is appreciable only over distances large compared with the dimensions  $r_0$  of the averaging region; this is certainly the case for fields whose wavelengths are in the visible part of the spectrum or longer. Since the integrand in (27.20) vanishes when  $\bar{\mathbf{r}}$  is more than  $r_0$  from  $\mathbf{r}$ , then if  $\mathbf{p}(\bar{\mathbf{r}})$  varies negligibly over a distance  $r_0$  from  $\bar{\mathbf{r}}$ , we can replace  $\mathbf{p}(\bar{\mathbf{r}})$  by  $\mathbf{p}(\mathbf{r})$ , and bring it outside the integral to obtain:

$$\mathbf{P}(\mathbf{r}) = \frac{\mathbf{p}(\mathbf{r})}{v} \int d\bar{\mathbf{r}} f(\mathbf{r} - \bar{\mathbf{r}}). \quad (27.21)$$

Since  $\int d\mathbf{r}' f(\mathbf{r}') = 1$ , we finally have

$$\mathbf{P}(\mathbf{r}) = \frac{1}{v} \mathbf{p}(\mathbf{r}); \quad (27.22)$$

i.e., provided the dipole moment of each cell varies appreciably only on the macroscopic scale, then the macroscopic Maxwell equation (27.4) holds with the polarization density  $\mathbf{P}(\mathbf{r})$  defined to be the dipole moment of a primitive cell in the neighborhood of  $\mathbf{r}$ , divided by its equilibrium volume.<sup>10</sup>

## THEORY OF THE LOCAL FIELD

To exploit macroscopic electrostatics, a theory is required relating the polarization density  $\mathbf{P}$  back to the macroscopic electric field  $\mathbf{E}$ . Since each ion has microscopic dimensions, its displacement and distortion will be determined by the force due to the *microscopic* field at the position of the ion, diminished by the contribution to the microscopic field from the ion itself. This field is frequently called the local (or effective) field,  $\mathbf{E}^{\text{loc}}(\mathbf{r})$ .

We can exploit macroscopic electrostatics to simplify the evaluation of  $\mathbf{E}^{\text{loc}}(\mathbf{r})$  by dividing space into regions near to and far from  $\mathbf{r}$ . The far region is to contain all external sources of field, all points outside the crystal, and only points inside the crystal that are far from  $\mathbf{r}$  compared with the dimensions  $r_0$  of the averaging region used in (Eq. (27.6)). All other points are said to be in the near region (Figure 27.3). The reason for this division is that the contribution to  $\mathbf{E}^{\text{loc}}(\mathbf{r})$  of all charge in the far region will vary negligibly over a distance  $r_0$  about  $\mathbf{r}$ , and would be unaffected if we were to apply the averaging procedure specified in (27.6). Therefore the contribution to  $\mathbf{E}^{\text{loc}}(\mathbf{r})$  of all charge in the far region is just the macroscopic field,  $\mathbf{E}_{\text{far}}^{\text{macro}}(\mathbf{r})$ , that would exist at  $\mathbf{r}$  if only the charge in the far region were present:

$$\mathbf{E}^{\text{loc}}(\mathbf{r}) = \mathbf{E}_{\text{near}}^{\text{loc}}(\mathbf{r}) + \mathbf{E}_{\text{far}}^{\text{micro}}(\mathbf{r}) = \mathbf{E}_{\text{near}}^{\text{loc}}(\mathbf{r}) + \mathbf{E}_{\text{far}}^{\text{macro}}(\mathbf{r}). \quad (27.23)$$

Now  $\mathbf{E}(\mathbf{r})$ , the full macroscopic field at  $\mathbf{r}$ , is constructed by averaging the microscopic field within  $r_0$  of  $\mathbf{r}$  due to all charges, in both the near and the far regions; i.e.,

$$\mathbf{E}(\mathbf{r}) = \mathbf{E}_{\text{far}}^{\text{macro}}(\mathbf{r}) + \mathbf{E}_{\text{near}}^{\text{macro}}(\mathbf{r}), \quad (27.24)$$

<sup>10</sup> The derivation of this intuitive result permits us to estimate corrections when required.

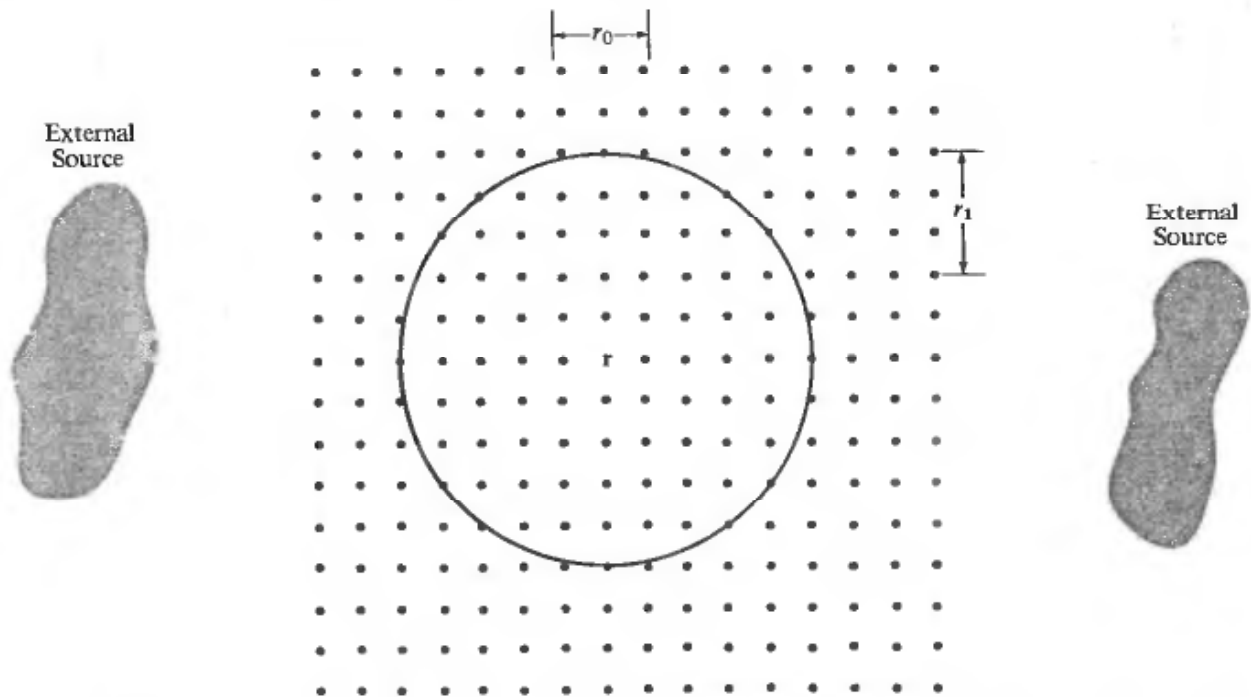


Figure 27.3

In calculating the local field at a point  $r$  it is convenient to consider separately contributions from the *far region* (i.e., all the crystal outside the sphere of radius  $r_1$  about  $r$  and all external sources of field) and from the *near region* (i.e., all points within the sphere about  $r$ ). The far region is taken to be far from  $r$  on the scale of the averaging length  $r_0$ , to insure that the microscopic field due to charges in the far region is equal to its macroscopic average.

where  $E_{\text{near}}^{\text{macro}}(\mathbf{r})$  is the macroscopic field that would exist at  $r$  if only the charges in the near region<sup>11</sup> were present. We can therefore rewrite Eq. (27.23) as:

$$E^{\text{loc}}(\mathbf{r}) = E(\mathbf{r}) + E_{\text{near}}^{\text{loc}}(\mathbf{r}) - E_{\text{near}}^{\text{macro}}(\mathbf{r}). \quad (27.25)$$

Thus we have related the unknown local field at  $r$  to the macroscopic electric field<sup>12</sup> at  $r$  and additional terms that depend only on the configuration of charges in the near region.

We shall apply (27.25) only to nonequilibrium configurations of the crystal with negligible spatial variation from cell to cell over distances of order  $r_1$ , the size of the near region.<sup>13</sup> In such cases  $E_{\text{near}}^{\text{macro}}(\mathbf{r})$  will be the macroscopic field due to a *uniformly* polarized medium, whose shape is that of the near region. If we choose the near region

<sup>11</sup> Including, of course, the ion on which we are calculating the force.

<sup>12</sup> A further complication of a purely macroscopic nature is peripheral to the argument here, in which  $E(\mathbf{r})$  is assumed to be given. If the internal field and polarization are produced by placing the sample in a specified field  $E^{\text{ext}}$ , then an additional problem in macroscopic electrostatics must be solved to determine the macroscopic field  $E$  in the interior of the sample, since the discontinuity in the polarization density  $\mathbf{P}$  at the surface of the sample acts as a bound surface charge, and contributes an additional term to the macroscopic field in the interior. For certain simply shaped samples in uniform external fields the induced polarization  $\mathbf{P}$  and the macroscopic field  $E$  in the interior will both be constant and parallel to  $E^{\text{ext}}$ , and one can write:  $E = E^{\text{ext}} - N\mathbf{P}$ , where  $N$ , the "depolarization factor," depends on the geometry of the sample. The most important elementary case is the sphere, for which  $N = 4\pi/3$ . For a general ellipsoid (in which  $\mathbf{P}$  need not be parallel to  $E$ ) see E. C. Stoner, *Phil. Mag.* **36**, 803 (1945).

<sup>13</sup> Note that we are now very macroscopic indeed, requiring that  $\lambda \gg r_1 \gg r_0 \gg a$ .

to be a sphere, then this field is given by the following elementary result of electrostatics (see Problem 1): The macroscopic field anywhere inside a uniformly polarized sphere is just  $\mathbf{E} = -4\pi\mathbf{P}/3$ , where  $\mathbf{P}$  is the polarization density. Therefore if the near region is a sphere over which  $\mathbf{P}$  has negligible spatial variation, then Eq. (27.25) becomes

$$\mathbf{E}^{\text{loc}}(\mathbf{r}) = \mathbf{E}(\mathbf{r}) + \mathbf{E}_{\text{near}}^{\text{loc}}(\mathbf{r}) + \frac{4\pi\mathbf{P}(\mathbf{r})}{3}. \quad (27.26)$$

We are thus left with the problem of calculating the microscopic local field  $\mathbf{E}_{\text{near}}^{\text{loc}}(\mathbf{r})$  appropriate to a spherical region whose center is taken to be the ion on which the field acts. Inside this region the charge density is the same in every cell (except for the removal of the ion at the center on which we are calculating the force). In most applications this calculation is done under the following simplifying assumptions:

1. The spatial dimensions and the displacement from equilibrium of each ion are considered to be so small that the polarizing field acting on it can be taken to be uniform over the whole ion and equal to the value of  $\mathbf{E}^{\text{loc}}$  at the equilibrium position of the ion.
2. The spatial dimensions and the displacement from equilibrium of each ion are considered to be so small that the contribution to the local field at the equilibrium position of the given ion, from the ion whose equilibrium position is  $\mathbf{R} + \mathbf{d}$ , is accurately given by the field of a dipole of moment  $e(\mathbf{d})\mathbf{u}(\mathbf{R} + \mathbf{d}) + \mathbf{p}(\mathbf{R} + \mathbf{d})$ .

Since the dipole moments of ions at equivalent sites (displaced from each other by Bravais lattice vectors  $\mathbf{R}$ ) are identical within the near region over which  $\mathbf{P}$  has negligible variation, the calculation of  $\mathbf{E}_{\text{near}}^{\text{loc}}$  at an equilibrium site reduces to the type of lattice sum we described in Chapter 20. Furthermore, in the special case in which every equilibrium site in the equilibrium crystal is a center of cubic symmetry, it is easily shown (Problem 2) that this lattice sum must vanish; i.e.,  $\mathbf{E}_{\text{near}}^{\text{loc}}(\mathbf{r}) = 0$  at every equilibrium site. Since this case includes both the solid noble gases and the alkali halides, it is the only one we consider. For these crystals we may assume that the field polarizing each ion in the neighborhood of  $\mathbf{r}$  is<sup>14</sup>

$$\mathbf{E}^{\text{loc}}(\mathbf{r}) = \mathbf{E}(\mathbf{r}) + \frac{4\pi\mathbf{P}(\mathbf{r})}{3}. \quad (27.27)$$

This result, sometimes known as the Lorentz relation, is widely used in theories of dielectrics. It is very important to remember the assumptions underlying it, particularly that of cubic symmetry about every equilibrium site.

Sometimes (27.27) is written in terms of the dielectric constant  $\epsilon$  of the medium, using the constitutive relation<sup>15</sup>

$$\mathbf{D}(\mathbf{r}) = \epsilon\mathbf{E}(\mathbf{r}), \quad (27.28)$$

<sup>14</sup> Note that implicit in this relation is the fact that the local field acting on an ion depends only on the general location of the ion but not (in a lattice with a basis) on the type of ion (i.e., it depends on  $\mathbf{R}$  but not on  $\mathbf{d}$ ). This convenient simplification is a consequence of our assumption that every ion occupies a position of cubic symmetry.

<sup>15</sup> In noncubic crystals  $\mathbf{P}$ , and therefore  $\mathbf{D}$ , need not be parallel to  $\mathbf{E}$ , so  $\epsilon$  is a tensor.

together with the relation (27.3) between  $\mathbf{D}$ ,  $\mathbf{E}$ , and  $\mathbf{P}$ , to express  $\mathbf{P}(\mathbf{r})$  in terms of  $\mathbf{E}(\mathbf{r})$ :

$$\mathbf{P}(\mathbf{r}) = \frac{\epsilon - 1}{4\pi} \mathbf{E}(\mathbf{r}). \quad (27.29)$$

Using this to eliminate  $\mathbf{P}(\mathbf{r})$  from (27.27), one finds that

$$\mathbf{E}^{\text{loc}}(\mathbf{r}) = \frac{\epsilon + 2}{3} \mathbf{E}(\mathbf{r}). \quad (27.30)$$

Yet another way of expressing the same result is in terms of the *polarizability*,  $\alpha$ , of the medium. The polarizability  $\alpha(\mathbf{d})$  of the type of ion at position  $\mathbf{d}$  in the basis is defined to be the ratio of its induced dipole moment to the field actually acting on it. Thus

$$\mathbf{p}(\mathbf{R} + \mathbf{d}) + e\mathbf{u}(\mathbf{R} + \mathbf{d}) = \alpha(\mathbf{d}) \mathbf{E}^{\text{loc}}(\mathbf{r})|_{\mathbf{r} \approx \mathbf{R}}. \quad (27.31)$$

The polarizability  $\alpha$  of the medium is defined as the sum of the polarizabilities of the ions in a primitive cell:

$$\alpha = \sum_{\mathbf{d}} \alpha(\mathbf{d}). \quad (27.32)$$

Since (cf. (27.18) and (27.22)),

$$\mathbf{P}(\mathbf{r}) = \frac{1}{v} \sum_{\mathbf{d}} \left[ \mathbf{p}(\mathbf{R}, \mathbf{d}) + e(\mathbf{d})\mathbf{u}(\mathbf{R}, \mathbf{d}) \right]_{\mathbf{R} \approx \mathbf{r}}, \quad (27.33)$$

it follows that

$$\mathbf{P}(\mathbf{r}) = \frac{\alpha}{v} \mathbf{E}^{\text{loc}}(\mathbf{r}). \quad (27.34)$$

Using (27.29) and (27.30) to express both  $\mathbf{P}$  and  $\mathbf{E}^{\text{loc}}$  in terms of  $\mathbf{E}$ , we find that (27.34) implies that

$$\frac{\epsilon - 1}{\epsilon + 2} = \frac{4\pi\alpha}{3v}. \quad (27.35)$$

This equation, known as the Clausius-Mossotti relation,<sup>16</sup> provides a valuable link between macroscopic and microscopic theories. A microscopic theory is required to calculate  $\alpha$ , which gives the response of the ions to the actual field  $\mathbf{E}^{\text{loc}}$  acting on them. The resulting  $\epsilon$  can then be used, in conjunction with the macroscopic Maxwell equations, to predict the optical properties of the insulator.

## THEORY OF THE POLARIZABILITY

Two terms contribute to the polarizability  $\alpha$ . The contribution from  $\mathbf{p}$  (see Eq. (27.31)), the "atomic polarizability," arises from the distortion of the ionic charge distribution.

<sup>16</sup> When written in terms of the index of refraction,  $n = \sqrt{\epsilon}$ , the Clausius-Mossotti relation is known as the Lorentz-Lorenz relation. (In the recent physics and chemistry literature of England and the United States it has become the widespread practice to misspell the last name of O. F. Mossotti with a single "s," and/or to interchange his initials.)

The contribution from  $\epsilon_u$ , the “displacement polarizability,” arises from ionic displacements. There is no displacement polarizability in molecular crystals where the “ions” are uncharged, but in ionic crystals it is comparable to the atomic polarizability.

### Atomic Polarizability

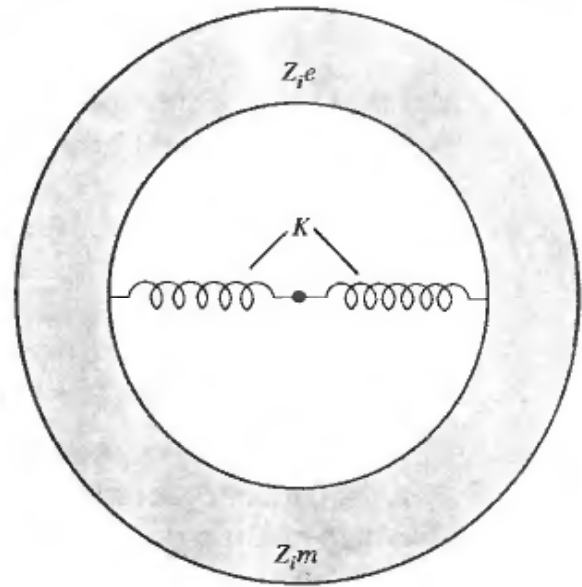
We allow the local field acting on the ion in question to be frequency-dependent, writing

$$\mathbf{E}^{\text{loc}} = \text{Re}(\mathbf{E}_0 e^{-i\omega t}), \quad (27.36)$$

where  $\mathbf{E}_0$  is independent of position (assumption 1, page 541). The simplest classical theory of atomic polarizability treats the ion as an electronic shell of charge  $Z_i e$  and mass  $Z_i m$  tied to a heavy, immobile, undeformable ion core, by a harmonic spring, of spring constant  $K = Z_i m \omega_0^2$  (Figure 27.4). If the displacement of the shell

**Figure 27.4**

Crude classical model of atomic polarizability. The ion is represented as a charged shell of charge  $Z_i e$  and mass  $Z_i m$  tied to an immobile nucleus by a spring of force constant  $K = Z_i m \omega_0^2$ .



from its equilibrium position is given by

$$\mathbf{r} = \text{Re}(\mathbf{r}_0 e^{-i\omega t}), \quad (27.37)$$

then the equation of motion of the shell,

$$Z_i m \ddot{\mathbf{r}} = -K\mathbf{r} - Z_i e \mathbf{E}^{\text{loc}}, \quad (27.38)$$

implies that

$$\mathbf{r}_0 = -\frac{e\mathbf{E}_0}{m(\omega_0^2 - \omega^2)}. \quad (27.39)$$

Since the induced dipole moment is  $\mathbf{p} = -Z_i e \mathbf{r}$ , we have

$$\mathbf{p} = \text{Re}(\mathbf{p}_0 e^{-i\omega t}), \quad (27.40)$$

with

$$\mathbf{p}_0 = \frac{Z_i e^2}{m(\omega_0^2 - \omega^2)} \mathbf{E}_0. \quad (27.41)$$

Defining the frequency-dependent atomic polarizability by

$$\mathbf{p}_0 = \alpha^{\text{at}}(\omega) \mathbf{E}_0, \quad (27.42)$$

we have

$$\alpha^{\text{at}}(\omega) = \frac{Z_i e^2}{m(\omega_0^2 - \omega^2)}. \quad (27.43)$$

The model leading to (27.43) is, of course, very crude. However, for our purposes the most important feature of the result is that if  $\omega$  is small compared with  $\omega_0$ , the polarizability will be independent of frequency and equal to its static value:

$$\alpha^{\text{at}} = \frac{Z_i e^2}{m\omega_0^2}. \quad (27.44)$$

We would expect  $\omega_0$ , the frequency of vibration of the electronic shell, to be of the order of an atomic excitation energy divided by  $\hbar$ . This suggests that, unless  $\hbar\omega$  is of the order of several electron volts, we can take the atomic polarizability to be independent of frequency. This is confirmed by more accurate quantum-mechanical calculations of  $\alpha$ .

Note that we can also use (27.44) to estimate the frequency below which  $\alpha^{\text{at}}$  will be frequency-independent, in terms of the observed static polarizabilities:

$$\begin{aligned} \hbar\omega_0 &= \sqrt{\frac{\hbar^2 Z_i e^2}{m\alpha^{\text{at}}}} \\ &= \sqrt{\frac{4a_0^3 Z_i}{\alpha^{\text{at}}} \frac{e^2}{2a_0}}, \quad a_0 = \frac{\hbar^2}{me^2}, \\ &= \sqrt{Z_i \left( \frac{10^{-24} \text{ cm}^3}{\alpha^{\text{at}}} \right)} \times 10.5 \text{ eV}. \end{aligned} \quad (27.45)$$

Since the measured polarizabilities (see Table 27.1) are of the order of  $10^{-24} \text{ cm}^3$ , we conclude that the frequency dependence of the atomic polarizability will not come into play (in all but the most highly polarizable of ions) until frequencies corresponding to ultraviolet radiation.

Table 27.1  
ATOMIC POLARIZABILITIES OF THE HALOGEN IONS,  
NOBLE GAS ATOMS, AND ALKALI METAL IONS<sup>a</sup>

HALOGENS		NOBLE GASES		ALKALI METALS	
		He	0.2	Li <sup>+</sup>	0.03
F <sup>-</sup>	1.2	Ne	0.4	Na <sup>+</sup>	0.2
Cl <sup>-</sup>	3	Ar	1.6	K <sup>+</sup>	0.9
Br <sup>-</sup>	4.5	Kr	2.5	Rb <sup>+</sup>	1.7
I <sup>-</sup>	7	Xe	4.0	Cs <sup>+</sup>	2.5

<sup>a</sup> In units of  $10^{-24} \text{ cm}^3$ . Note that entries in the same row have the same electronic shell structure, but increasing nuclear charge.  
Source: A. Dalgarno, *Advances Phys.* **11**, 281 (1962).

### Displacement Polarizability

In ionic crystals we must consider the dipole moment due to the displacement of the charged ions by the electric field, in addition to the atomic polarization resulting



from the deformation of their electronic shells by the field. We begin by ignoring the atomic polarization (*rigid-ion approximation*). To simplify the discussion we also consider only crystals with two ions per primitive cell, of charges  $e$  and  $-e$ . If the ions are undeformable, then the dipole moment of the primitive cell is just

$$\mathbf{p} = e\mathbf{w}, \quad \mathbf{w} = \mathbf{u}^+ - \mathbf{u}^-, \quad (27.46)$$

where  $\mathbf{u}^\pm$  is the displacement of the positive or negative ion from its equilibrium position.

To determine  $\mathbf{w}(\mathbf{r})$  we note that the long-range electrostatic forces between ions are already contained in the field  $\mathbf{E}^{\text{loc}}$ . The remaining short-range interionic forces (e.g., higher-order electrostatic multipole moments and core-core repulsion) will fall off rapidly with distance, and we may assume that they produce a restoring force for an ion at  $\mathbf{r}$  that depends only on the displacement of the ions in its vicinity. Since we are considering disturbances that vary slowly on the atomic scale, in the vicinity of  $\mathbf{r}$  all ions of the same charge move as a whole with the same displacement,  $\mathbf{u}^+(\mathbf{r})$  or  $\mathbf{u}^-(\mathbf{r})$ . Thus the short-range part of the restoring force acting on an ion at  $\mathbf{r}$  will simply be proportional to<sup>17</sup> the relative displacement  $\mathbf{w}(\mathbf{r}) = \mathbf{u}^+(\mathbf{r}) - \mathbf{u}^-(\mathbf{r})$  of the two oppositely charged sublattices in the neighborhood of  $\mathbf{r}$ .

Consequently in a distortion of the crystal with slow spatial variation on the microscopic scale, the displacements of the positive and negative ions satisfy equations of the form:

$$\begin{aligned} M_+ \ddot{\mathbf{u}}^+ &= -k(\mathbf{u}^+ - \mathbf{u}^-) + e\mathbf{E}^{\text{loc}}, \\ M_- \ddot{\mathbf{u}}^- &= -k(\mathbf{u}^- - \mathbf{u}^+) - e\mathbf{E}^{\text{loc}}, \end{aligned} \quad (27.47)$$

which can be written

$$\dot{\mathbf{w}} = \frac{e}{M} \mathbf{E}^{\text{loc}} - \frac{k}{M} \mathbf{w}, \quad (27.48)$$

where  $M$  is the ionic reduced mass,  $M^{-1} = (M_+)^{-1} + (M_-)^{-1}$ . Letting  $\mathbf{E}^{\text{loc}}$  be an AC field of the form (27.36), we find that

$$\mathbf{w} = \text{Re}(\mathbf{w}_0 e^{-i\omega t}), \quad \mathbf{w}_0 = \frac{e\mathbf{E}_0/M}{\bar{\omega}^2 - \omega^2}, \quad (27.49)$$

where

$$\bar{\omega}^2 = \frac{k}{M}. \quad (27.50)$$

Accordingly,

$$\alpha^{\text{dis}} = \frac{p_0}{E_0} = \frac{e\mathbf{w}_0}{E_0} = \frac{e^2}{M(\bar{\omega}^2 - \omega^2)}. \quad (27.51)$$

Note that the displacement polarizability (27.51) has the same form as the atomic polarizability (27.43). However the resonant frequency  $\bar{\omega}$  is characteristic of lattice vibrational frequencies, and therefore  $\hbar\bar{\omega} \approx \hbar\omega_D \approx 10^{-1}$  to  $10^{-2}$  eV. This can be  $10^2$  to  $10^3$  times smaller than the atomic frequency  $\omega_0$ , and therefore, in contrast to the atomic polarizability, the displacement polarizability has a significant frequency dependence in the infrared and optical range.

<sup>17</sup> The proportionality constant in general will be a tensor, but it reduces to a constant in a crystal of cubic symmetry, the only case we consider here.

Note also that because the ionic mass  $M$  is about  $10^4$  times the electronic mass  $m$ , the static ( $\omega = 0$ ) ionic and displacement polarizabilities may well be of the same size. This means that the rigid-ion model we have used is unjustifiable, and (27.51) must be corrected to take into account the atomic polarizability of the ions as well. The most naive way to do this is simply to add the two types of contribution to the polarizability:

$$\alpha = (\alpha^+ + \alpha^-) + \frac{e^2}{M(\bar{\omega}^2 - \omega^2)}, \quad (27.52)$$

where  $\alpha^+$  and  $\alpha^-$  are the atomic polarizabilities of the positive and negative ions. There is no real justification for this, since the first term in (27.52) was calculated on the assumption that the ions were immobile but polarizable, while the second was calculated for ions that could be moved, but not deformed. Evidently a more reasonable approach would combine the models that lead on the one hand to (27.43) and, on the other, to (27.51), calculating in one step the response to the local field of ions that can be both displaced and deformed. Such theories are known as *shell model* theories. They generally lead to results that differ considerably in numerical detail from those predicted by the more naive (27.52), but have many of the same basic structural features. We therefore explore the consequences of (27.52) further, indicating later how it should be modified in a more reasonable model.

In conjunction with the Clausius-Mossotti relation (27.35), the approximation expressed by (27.52) leads to a dielectric constant  $\epsilon(\omega)$  for an ionic crystal, given by

$$\frac{\epsilon(\omega) - 1}{\epsilon(\omega) + 2} = \frac{4\pi}{3v} \left( \alpha^+ + \alpha^- + \frac{e^2}{M(\bar{\omega}^2 - \omega^2)} \right). \quad (27.53)$$

In particular, the static dielectric constant is given by

$$\frac{\epsilon_0 - 1}{\epsilon_0 + 2} = \frac{4\pi}{3v} \left( \alpha^+ + \alpha^- + \frac{e^2}{M\bar{\omega}^2} \right), \quad (\omega \ll \bar{\omega}), \quad (27.54)$$

while the high-frequency<sup>18</sup> dielectric constant satisfies

$$\frac{\epsilon_\infty - 1}{\epsilon_\infty + 2} = \frac{4\pi}{3v} (\alpha^+ + \alpha^-), \quad (\bar{\omega} \ll \omega \ll \omega_0). \quad (27.55)$$

It is convenient to write  $\epsilon(\omega)$  in terms of  $\epsilon_0$  and  $\epsilon_\infty$ , since the two limiting forms are readily measured:  $\epsilon_0$  is the static dielectric constant of the crystal, while  $\epsilon_\infty$  is the dielectric constant at optical frequencies, and is therefore related to the index of refraction,  $n$ , by  $n^2 = \epsilon_\infty$ . We have

$$\frac{\epsilon(\omega) - 1}{\epsilon(\omega) + 2} = \frac{\epsilon_\infty - 1}{\epsilon_\infty + 2} + \frac{1}{1 - (\omega^2/\bar{\omega}^2)} \left( \frac{\epsilon_0 - 1}{\epsilon_0 + 2} - \frac{\epsilon_\infty - 1}{\epsilon_\infty + 2} \right), \quad (27.56)$$

<sup>18</sup> In this context, by "high frequencies" we shall always mean frequencies high compared with lattice vibrational frequencies, but low compared with atomic excitation frequencies. The frequency of visible light generally satisfies this condition.

which can be solved for  $\epsilon(\omega)$ :

$$\epsilon(\omega) = \epsilon_\infty + \frac{\epsilon_\infty - \epsilon_0}{(\omega^2/\omega_T^2) - 1}, \quad (27.57)$$

where

$$\omega_T^2 = \bar{\omega}^2 \left( \frac{\epsilon_\infty + 2}{\epsilon_0 + 2} \right) = \bar{\omega}^2 \left( 1 - \frac{\epsilon_0 - \epsilon_\infty}{\epsilon_0 + 2} \right). \quad (27.58)$$

### Application to Long-Wavelength Optical Modes of Ionic Crystals

To calculate the normal mode dispersion relations in an ionic crystal we could proceed by the general techniques described in Chapter 22. However, we would encounter severe computational difficulties because of the very long range of the interionic electrostatic interactions. Techniques have been developed for dealing with this problem, similar to those exploited in calculating the cohesive energy of an ionic crystal (Chapter 20). However, for long-wavelength optical modes one can avoid such calculations by stating the problem as one in macroscopic electrostatics:

In a long-wavelength ( $\mathbf{k} \approx 0$ ) optical mode the oppositely charged ions in each primitive cell undergo oppositely directed displacements, giving rise to a non-vanishing polarization density  $\mathbf{P}$ . Associated with this polarization density there will in general be a macroscopic electric field  $\mathbf{E}$  and an electric displacement  $\mathbf{D}$ , related by

$$\mathbf{D} = \epsilon\mathbf{E} = \mathbf{E} + 4\pi\mathbf{P}. \quad (27.59)$$

In the absence of free charge, we have

$$\nabla \cdot \mathbf{D} = 0. \quad (27.60)$$

Furthermore,  $\mathbf{E}^{\text{micro}}$  is the gradient of a potential.<sup>19</sup> It follows from (27.6) that  $\mathbf{E}$  is also, so that

$$\nabla \times \mathbf{E} = \nabla \times (-\nabla\phi) = 0. \quad (27.61)$$

In a cubic crystal  $\mathbf{D}$  is parallel to  $\mathbf{E}$  (i.e.,  $\epsilon$  is not a tensor) and therefore, from (27.59), both are parallel to  $\mathbf{P}$ . If all three have the spatial dependence,

$$\begin{Bmatrix} \mathbf{D} \\ \mathbf{E} \\ \mathbf{P} \end{Bmatrix} = \text{Re} \begin{Bmatrix} \mathbf{D}_0 \\ \mathbf{E}_0 \\ \mathbf{P}_0 \end{Bmatrix} e^{i\mathbf{k} \cdot \mathbf{r}}, \quad (27.62)$$

then (27.60) reduces to  $\mathbf{k} \cdot \mathbf{D}_0 = 0$ , which requires that

$$\mathbf{D} = 0 \quad \text{or} \quad \mathbf{D}, \mathbf{E}, \text{ and } \mathbf{P} \perp \mathbf{k}, \quad (27.63)$$

while (27.61) reduces to  $\mathbf{k} \times \mathbf{E}_0 = 0$ , which requires that

$$\mathbf{E} = 0 \quad \text{or} \quad \mathbf{E}, \mathbf{D}, \text{ and } \mathbf{P} \parallel \mathbf{k}. \quad (27.64)$$

In a longitudinal optical mode the (nonzero) polarization density  $\mathbf{P}$  is parallel to  $\mathbf{k}$ ,

<sup>19</sup> At optical frequencies one might worry about keeping only electrostatic fields, since the right side of the full Maxwell equation,  $\nabla \times \mathbf{E} = -(1/c) \partial \mathbf{B} / \partial t$  need not be negligible. We shall see shortly, however, that a full electrodynamic treatment leads to very much the same conclusions.

and Eq. (27.63) therefore requires that  $\mathbf{D}$  must vanish. This is consistent with (27.59) only if

$$\mathbf{E} = -4\pi\mathbf{P}, \quad \epsilon = 0 \quad (\text{longitudinal mode}). \quad (27.65)$$

On the other hand, in a transverse optical mode the (nonzero) polarization density  $\mathbf{P}$  is perpendicular to  $\mathbf{k}$ , which is consistent with (27.64) only if  $\mathbf{E}$  vanishes. This, however, is consistent with (27.59) only if

$$\mathbf{E} = 0, \quad \epsilon = \infty \quad (\text{transverse mode}). \quad (27.66)$$

According to (27.57),  $\epsilon = \infty$  when  $\omega^2 = \omega_T^2$ , and therefore the result (27.66) identifies  $\omega_T$  as the frequency of the long-wavelength ( $\mathbf{k} \rightarrow 0$ ) transverse optical mode. The frequency  $\omega_L$  of the longitudinal optical mode is determined by the condition  $\epsilon = 0$  (Eq. (27.65)), and (27.57) therefore gives

$$\boxed{\omega_L^2 = \frac{\epsilon_0}{\epsilon_\infty} \omega_T^2.} \quad (27.67)$$

This equation, relating the longitudinal and transverse optical-mode frequencies to the static dielectric constant and index of refraction, is known as the *Lyddane-Sachs-Teller relation*. Note that it follows entirely from the interpretation that (27.65) and (27.66) lend to the zeros and poles of  $\epsilon(\omega)$ , together with the functional form of (27.57)—i.e., the fact that in the frequency range of interest  $\epsilon$  as a function of  $\omega^2$  is a constant plus a simple pole. As a result, the relation has a validity going well beyond the crude approximation (27.52) of additive polarizabilities, and also applies to the far more sophisticated shell model theories of diatomic ionic crystals.

Since the crystal is more polarizable at low frequencies<sup>20</sup> than at high,  $\omega_L$  exceeds  $\omega_T$ . It may seem surprising that  $\omega_L$  should differ at all from  $\omega_T$  in the limit of long wavelengths, since in this limit the ionic displacements in any region of finite extent are indistinguishable. However, because of the long range of electrostatic forces, their influence can always persist over distances comparable to the wavelength, no matter how long that wavelength may be; thus longitudinal and transverse optical modes will always experience different electrostatic restoring forces.<sup>21</sup> Indeed, if we use the Lorentz relation (27.27) we find from (27.65) that the electrostatic restoring force in a long-wavelength longitudinal optical mode is given by the local field

$$(\mathbf{E}^{\text{loc}})_L = \mathbf{E} + \frac{4\pi\mathbf{P}}{3} = -\frac{8\pi\mathbf{P}}{3} \quad (\text{longitudinal}), \quad (27.68)$$

while (from (27.66)) it is given in a long-wavelength transverse optical mode by

$$(\mathbf{E}^{\text{loc}})_T = \frac{4\pi\mathbf{P}}{3} \quad (\text{transverse}). \quad (27.69)$$

<sup>20</sup> At frequencies well above the natural vibrational frequencies of the ions, they fail to respond to an oscillatory force, and one has only atomic polarizability. At low frequencies both mechanisms can contribute.

<sup>21</sup> This argument, based on instantaneous action at a distance, must be reexamined when the electrostatic approximation (27.61) is dropped (see footnotes 19 and 25).

Thus in a longitudinal mode the local field acts to reduce the polarization (i.e., it adds to the short-range restoring force proportional to  $k = M\omega^2$ ) while in a transverse mode it acts to support the polarization (i.e., it reduces the short-range restoring force). This is consistent with (27.58), which predicts that  $\omega_T$  is less than  $\bar{\omega}$  (since  $\epsilon_0 - \epsilon_\infty$  is positive). It is also consistent with (27.67), which, with the aid of (27.58), can be written:

$$\omega_L^2 = \bar{\omega}^2 \left( 1 + 2 \frac{\epsilon_0 - \epsilon_\infty}{\epsilon_0 + 2\epsilon_\infty} \right), \quad (27.70)$$

which indicates that  $\omega_L$  exceeds  $\bar{\omega}$ .

The Lyddane-Sachs-Teller relation (27.67) has been confirmed by comparing measurements of  $\omega_L$  and  $\omega_T$  from neutron scattering, with measured values of the dielectric constant and index of refraction. In two alkali halides (NaI and KBr),  $\omega_L/\omega_T$  and  $(\epsilon_0/\epsilon_\infty)^{1/2}$  were found to agree to within the experimental uncertainty of the measurements (a few percent).<sup>22</sup>

However, because it is merely a consequence of the analytic form of  $\epsilon(\omega)$ , the validity of the Lyddane-Sachs-Teller relation does not provide a very stringent test of a theory. A more specific prediction can be constructed from Eqs. (27.54), (27.55), and (27.58), which combine together to give

$$\frac{9(\epsilon_0 - \epsilon_\infty)}{4\pi(\epsilon_\infty + 2)^2} \omega_T^2 = \frac{e^2}{Mv}. \quad (27.71)$$

Since  $e^2/Mv$  is determined entirely by the ionic charge, the ionic reduced mass, and the lattice constant, the right side of (27.71) is known. However, measured values of  $\epsilon_0$ ,  $\epsilon_\infty$ , and  $\omega_T$  in the alkali halides lead to a value for the left side of (27.71) that can be expressed in the form  $(e^*)^2/Mv$ , where  $e^*$  (known as the *Szigeti charge*) ranges between about  $0.7e$  and  $0.9e$ . This should *not* be taken as evidence that the ions are not fully charged, but as a telling sign of the failure of the crude assumption (27.52) that atomic and displacement polarizabilities simply add to give the total polarizability.

To remedy this defect, one must turn to a shell model theory in which atomic and displacement polarizations are calculated together, by allowing the electronic shell to move relative to the ion core (as done above in calculating the atomic polarizability) at the same time as the ion cores are themselves displaced.<sup>23</sup> The general structural form (27.57) of  $\epsilon(\omega)$  is preserved in such a theory, but the specific forms for the constants  $\epsilon_0$ ,  $\epsilon_\infty$ , and  $\omega_T$  can be quite different.

### Application to the Optical Properties of Ionic Crystals

The above discussion of the transverse optical mode is not completely accurate, based as it is on the electrostatic approximation (27.61) to the Maxwell equation:<sup>24</sup>

$$\nabla \times \mathbf{E} = -\frac{1}{c} \frac{\partial \mathbf{B}}{\partial t}. \quad (27.72)$$

<sup>22</sup> A. D. B. Woods et al., *Phys. Rev.* **131**, 1025 (1963).

<sup>23</sup> An early and particularly simple model is given by S. Roberts, *Phys. Rev.* **77**, 258 (1950).

<sup>24</sup> Our discussion of the longitudinal optical mode is founded entirely on the Maxwell equation  $\nabla \cdot \mathbf{D} = 0$  and remains valid in a fully electrodynamic analysis.

When (27.61) is replaced by the more general (27.72), the conclusion (27.66) that the transverse optical mode frequency is determined by the condition  $\epsilon(\omega) = \infty$  must be replaced by the more general result (Eq. (1.34)) that transverse fields with angular frequency  $\omega$  and wave vector  $\mathbf{k}$  can propagate only if

$$\epsilon(\omega) = \frac{k^2 c^2}{\omega^2}. \quad (27.73)$$

Thus for optical modes with wave vectors satisfying  $kc \gg \omega$ , the approximation  $\epsilon = \infty$  is reasonable. The frequencies of optical phonons are of order  $\omega_D = k_D s$ , where  $s$  is the speed of sound in the crystal, so this requires that

$$\frac{k}{k_D} \gg \frac{s}{c}. \quad (27.74)$$

Since  $k_D$  is comparable to the dimensions of the Brillouin zone, while  $s/c$  is of order  $10^{-4}$  to  $10^{-5}$ , the electrostatic approximation is fully justified except for optical modes whose wave vectors are only a small fraction of a percent of the dimensions of the zone from  $\mathbf{k} = 0$ .

We can describe the structure of the transverse modes all the way down to  $\mathbf{k} = 0$ , by plotting  $\epsilon$  vs.  $\omega$  (Eq. (27.57)) (Figure 27.5). Note that  $\epsilon$  is negative between  $\omega_T$  and  $\omega_L$ , so Eq. (27.73) requires  $kc$  to be imaginary. Thus no radiation can propagate in the crystal between the transverse and longitudinal optical frequencies. Outside this forbidden range  $\omega$  is plotted vs.  $k$  in Figure 27.6. The dispersion relation has two branches, lying entirely below  $\omega_T$  and entirely above  $\omega_L$ . The lower branch has the form  $\omega \equiv \omega_T$  except when  $k$  is so small as to be comparable to  $\omega_T/c$ . It describes the electric field accompanying a transverse optical mode in the constant-frequency region. However, when  $k$  is of order  $\omega_T/c$  the frequency falls below  $\omega_T$ , vanishing as  $kc/\sqrt{\epsilon_0}$ , a relation characteristic of ordinary electromagnetic radiation in a medium with dielectric constant  $\epsilon_0$ .

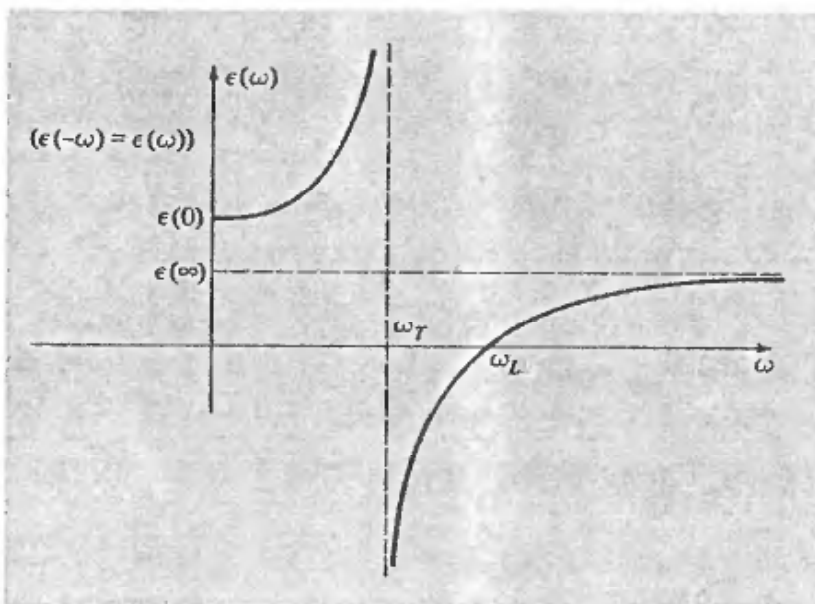
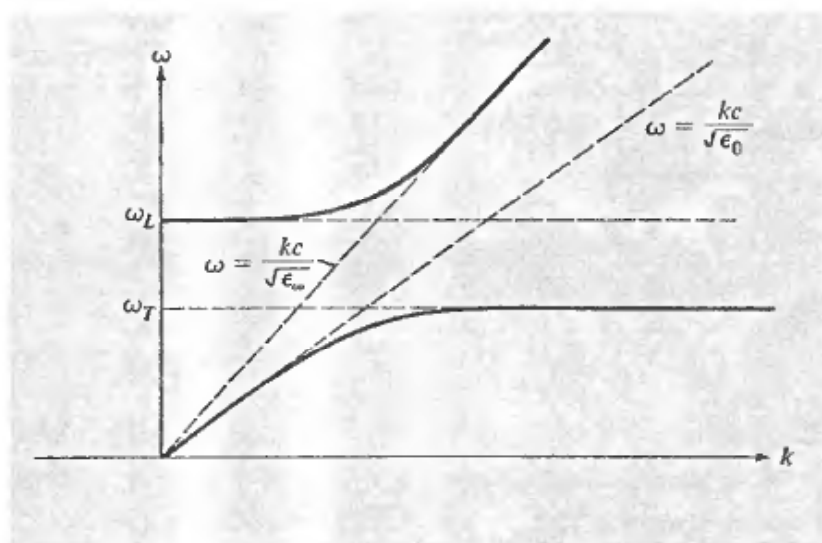


Figure 27.5  
Frequency-dependent dielectric constant for a diatomic ionic crystal.

Figure 27.6

Solutions to the dispersion relation  $\omega = kc/\sqrt{\epsilon(\omega)}$  for transverse electromagnetic modes propagating in a diatomic ionic crystal. (The relation to Figure 27.5 is most readily seen by rotating the figure through  $90^\circ$  and considering it to be a plot of  $k = \omega\sqrt{\epsilon(\omega)}/c$ , vs.  $\omega$ .) In the linear regions one mode is clearly photonlike and one clearly optical phononlike. In the curved regions both modes have a mixed nature, and are sometimes referred to as "polaritons."



The upper branch, on the other hand, assumes the linear form  $\omega = kc/\sqrt{\epsilon_\infty}$ , characteristic of electromagnetic radiation in a medium with dielectric constant  $\epsilon_\infty$ , when  $k$  is large compared with  $\omega_T/c$ , but as  $k$  approaches zero, the frequency does not vanish linearly, but levels off to  $\omega_L$ .<sup>25</sup>

Finally, note that if the dielectric constant is a real number, then the reflectivity of the crystal is given by (see Eq. (K.6) in Appendix K)

$$r = \left( \frac{\sqrt{\epsilon} - 1}{\sqrt{\epsilon} + 1} \right)^2. \quad (27.75)$$

As  $\epsilon \rightarrow \infty$ , the reflectivity approaches unity. Thus all incident radiation should be perfectly reflected at the frequency of the transverse optical mode. This effect can be amplified by repeated reflections of a ray from crystal faces. Since  $n$  reflections will diminish the intensity by  $r^n$ , after very many reflections only the component of radiation with frequencies very close to  $\omega_T$  will survive. This surviving radiation is known as the *reststrahl* (residual ray). Such repeated reflections provide a very precise way of measuring  $\omega_T$ , as well as a method for producing very monochromatic radiation in the infrared.

<sup>25</sup> Thus as  $k \rightarrow 0$  a transverse mode *does* occur at the same frequency as the longitudinal mode (see page 548). The reason this behavior emerges in an electrodynamic, but not an electrostatic, analysis is basically the finite velocity of signal propagation in an electrodynamic theory. Electromagnetic signals can only propagate with the speed of light, and therefore no matter how long their spatial range, they can be effective in distinguishing longitudinal from transverse modes only if they can travel a distance comparable to a wavelength in a time small compared with a period (i.e.,  $kc \gg \omega$ ). The argument on page 548, which explains why  $\omega_L$  and  $\omega_T$  differ, implicitly assumes that Coulomb forces act instantaneously at a distance, and becomes invalid when this assumption fails.

To the extent that the lattice vibrations are anharmonic (and therefore damped)  $\epsilon$  will also have an imaginary part. This broadens the reststrahl resonance. The typical behavior of observed frequency-dependent dielectric constants in ionic crystals, as deduced from their optical properties, is shown in Figure 27.7. Alkali halide dielectric properties are summarized in Table 27.2.

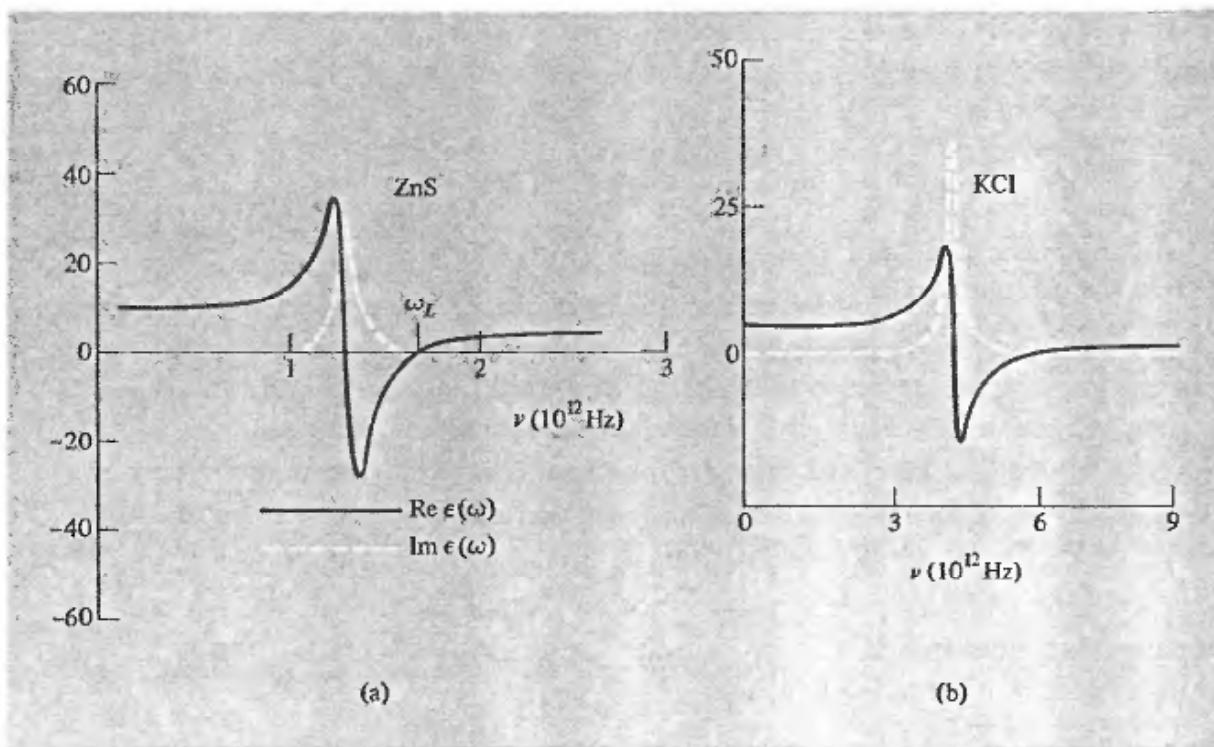


Figure 27.7

(a) Real (solid line) and imaginary (dashed line) parts of the dielectric constant of zinc sulfide. (After F. Abeles and J. P. Mathieu, *Annales de Physique* 3, 5 (1958); quoted by E. Burstein, *Phonons and Phonon Interactions*, T. A. Bak, ed., W. A. Benjamin, Menlo Park, California, 1964.) (b) Real (solid line) and imaginary (dashed line) parts of the dielectric constant of potassium chloride. (After G. R. Wilkinson and C. Smart; quoted by D. H. Martin, *Advances Phys.* 14, 39 (1965).)

## COVALENT INSULATORS

The above analysis of ionic and molecular crystals has relied on the possibility of resolving the charge distribution of the crystal into contributions from identifiable ions (atoms, molecules) as in (27.9). In covalent crystals, however, appreciable electronic charge density resides between ions (forming the so-called covalent bonds). This part of the total charge distribution is uniquely a property of the condensed state of matter, bearing no resemblance to the charge distribution of single isolated ions (atoms, molecules). Furthermore, since it comes from the most loosely bound atomic electrons, it makes a very important contribution to the polarizability of the crystal. Therefore, in calculating dielectric properties of covalent crystals one must deal with the polarizability of the crystal as a whole, either invoking band theory from the start or developing a phenomenology of "bond polarizabilities."

We shall not pursue this subject here, except to point out that covalent crystals can have quite large dielectric constants, reflecting the relatively delocalized structure of their electronic charge distributions. Static dielectric constants for selected covalent crystals are listed in Table 27.3. As we shall see (Chapter 28), the fac t the dielectric



Table 27.2  
 STATIC DIELECTRIC CONSTANT, OPTICAL DIELECTRIC  
 CONSTANT, AND TRANSVERSE OPTICAL PHONON  
 FREQUENCY FOR ALKALI HALIDE CRYSTALS

COMPOUND	$\epsilon_0$	$\epsilon_\infty$	$\hbar\omega_T/k_B^a$
LiF	9.01	1.96	442
NaF	5.05	1.74	354
KF	5.46	1.85	274
RbF	6.48	1.96	224
CsF	—	2.16	125
LiCl	11.95	2.78	276
NaCl	5.90	2.34	245
KCl	4.84	2.19	215
RbCl	4.92	2.19	183
CsCl	7.20	2.62	151
LiBr	13.25	3.17	229
NaBr	6.28	2.59	195
KBr	4.90	2.34	166
RbBr	4.86	2.34	139
CsBr	6.67	2.42	114
LiI	16.85	3.80	—
NaI	7.28	2.93	167
KI	5.10	2.62	156
RbI	4.91	2.59	117.5
CsI	6.59	2.62	94.6

<sup>a</sup> From the reststrahl peak; in degrees Kelvin.

Source: R. S. Knox and K. J. Teegarden, *Physics of Color Centers*, W. B. Fowler, ed., Academic Press, New York, 1968, page 625.

Table 27.3  
 STATIC DIELECTRIC CONSTANTS FOR SELECTED COVALENT AND  
 COVALENT-IONIC CRYSTALS OF THE DIAMOND, ZINCBLLENDE,  
 AND WURTZITE STRUCTURES<sup>a</sup>

CRYSTAL	STRUCTURE	$\epsilon_0$	CRYSTAL	STRUCTURE	$\epsilon_0$
C	<i>d</i>	5.7	ZnO	<i>w</i>	4.6
Si	<i>d</i>	12.0	ZnS	<i>w</i>	5.1
Ge	<i>d</i>	16.0	ZnSe	<i>z</i>	5.8
Sn	<i>d</i>	23.8	ZnTe	<i>z</i>	8.3
SiC	<i>z</i>	6.7	CdS	<i>w</i>	5.2
GaP	<i>z</i>	8.4	CdSe	<i>w</i>	7.0
GaAs	<i>z</i>	10.9	CdTe	<i>z</i>	7.1
GaSb	<i>z</i>	14.4	BeO	<i>w</i>	3.0
InP	<i>z</i>	9.6	MgO	<i>z</i>	3.0
InAs	<i>z</i>	12.2			
InSb	<i>z</i>	15.7			

<sup>a</sup> Quoted by J. C. Phillips, *Phys. Rev. Lett.* **20**, 550 (1968).

constants can be quite substantial is a point of considerable importance in the theory of impurity levels in semiconductors.

## PYROELECTRICITY

In deriving the macroscopic equation

$$\nabla \cdot \mathbf{E} = -4\pi \nabla \cdot \mathbf{P} \quad (27.76)$$

for ionic crystals, we assumed (see footnote 9) that the equilibrium dipole moment of the primitive cell,

$$\mathbf{p}_0 = \sum_{\mathbf{d}} \mathbf{d}e(\mathbf{d}), \quad (27.77)$$

vanished, and therefore ignored a term

$$\Delta \mathbf{P} = \frac{\mathbf{p}_0}{v} \quad (27.78)$$

in the polarization density  $\mathbf{P}$ . As Figure 27.8 demonstrates, the value of the dipole moment  $\mathbf{p}_0$  is not independent of the choice of primitive cell. However, since only the divergence of  $\mathbf{P}$  has physical significance, an additive constant vector  $\Delta \mathbf{P}$  does not affect the physics implied by the macroscopic Maxwell equations.

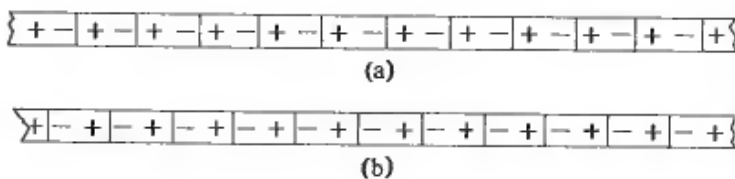


Figure 27.8

The dipole moment of the primitive cell depends on the choice of primitive cell. This is illustrated for a one-dimensional ionic crystal.

There would be nothing more to say if all crystals were infinite in extent. However, real crystals have surfaces, at which the macroscopic polarization density  $\mathbf{P}$  drops discontinuously to zero, thereby contributing a singular term on the right side of (27.76). This term is conventionally interpreted as a bound surface charge per unit area, whose magnitude is the normal component of  $\mathbf{P}$  at the surface,  $P_n$ . Thus an additive constant in  $\mathbf{P}$  is far from inconsequential in a finite crystal.

In a finite crystal, however, we must reexamine our assumption that each primitive cell has zero total charge:

$$\sum_{\mathbf{d}} e(\mathbf{d}) = 0. \quad (27.79)$$

In an infinite crystal of identical cells this is merely the statement that the crystal as a whole is neutral, but in a crystal with surfaces, only the interior cells are identically occupied, and charge neutrality is perfectly consistent with partially filled, and therefore charged, surface cells (Figure 27.9). Should one's choice of cell lead to surface cells containing net charge, an additional term would have to be added to (27.76) to represent this bound surface charge,  $\rho_s$ . When the choice of cell is changed, both  $P_n$  and  $\rho_s$  will change, in such a way that the total net macroscopic surface charge density,  $P_n + \rho_s$ , is unchanged.

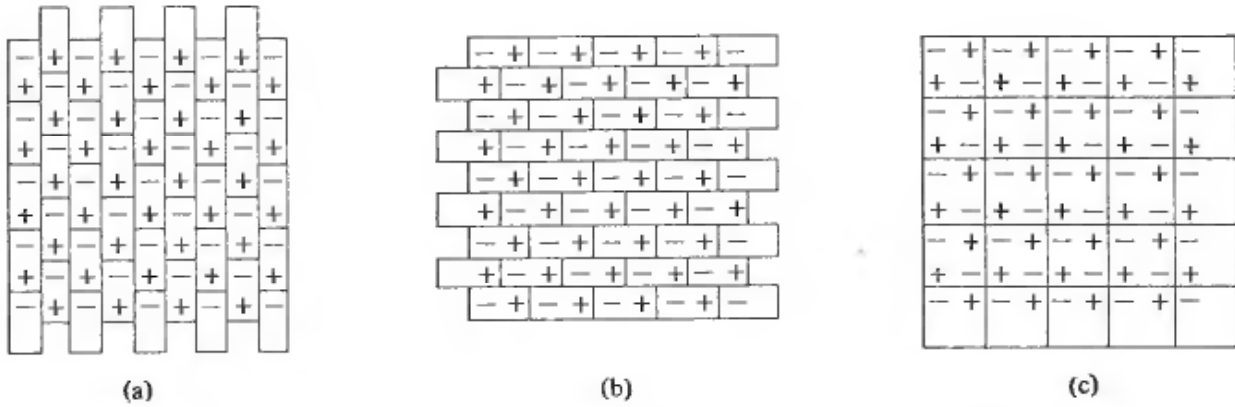


Figure 27.9

The “natural” choice of primitive cell is one that leads to uncharged cells at the surface. The cells chosen in (a) and (b) violate this criterion, and their contribution to the polarization density is cancelled by the contribution from the charged surface cells. The cell in (c) (which is non-primitive) leads to uncharged surface cells and has no dipole moment.

Thus the “natural” choice of cell for which (27.76) is valid without an additional term representing the unbalanced charge in surface cells, is a cell whose neutrality is maintained even at the surfaces of actual physical specimens.<sup>26</sup>

Crystals whose natural primitive cells have a nonvanishing dipole moment  $\mathbf{p}_0$  are called *pyroelectric*.<sup>27</sup> In equilibrium a perfect specimen of a pyroelectric crystal has a total dipole moment of  $\mathbf{p}_0$  times the number of cells in the crystal,<sup>28</sup> and thus a polarization density  $\mathbf{P} = \mathbf{p}_0/v$  throughout the crystal, even in the absence of an external field. This immediately implies some severe restrictions on the point-group symmetries of a pyroelectric crystal, for a symmetry operation must preserve all crystalline properties and, in particular, the direction of  $\mathbf{P}$ . Thus the only possible rotation axis is one parallel to  $\mathbf{P}$ , and furthermore there cannot be mirror planes perpendicular to that axis. This excludes all point groups except (Table 7.3)  $C_n$  and  $C_{nv}$  ( $n = 2, 3, 4, 6$ ) and  $C_1$  and  $C_{1h}$ . A glance at Table 7.3 reveals that these are the only point groups compatible with the location of a directed object (an arrow, for example) at each site.<sup>29</sup>

<sup>26</sup> This often requires a cell that is not primitive (see Figure 27.9), but it is easily verified that the earlier analysis in this chapter is in no way affected by using a larger microscopic cell.

<sup>27</sup> The name (pyro = fire) reflects the fact that under ordinary conditions the moment of a pyroelectric crystal will be masked by neutralizing layers of ions from the atmosphere that collect on the faces of the crystal. If, however, the crystal is heated, then the masking will no longer be complete, since the polarization will change due to thermal expansion of the crystal, neutralizing ions will be evaporated, etc. Thus the effect was first thought to be the production of an electric moment by heat. (Sometimes the term “polar crystal” is used instead of “pyroelectric crystal.” However, “polar crystal” is also widely used as a synonym for “ionic crystal” (whether pyroelectric or not), and the term is therefore best avoided.) The net polarization can also be masked by a domain structure, as in ferromagnets (see Chapter 33).

<sup>28</sup> The dipole moment of the surface cells need not be  $\mathbf{p}_0$ , but in the limit of a large crystal this will have a negligible effect on the total dipole moment, since the overwhelming majority of cells will be in the interior.

<sup>29</sup> Some crystals, though nonpyroelectric in the absence of external stresses can develop a spontaneous dipole moment when mechanically strained; i.e., by suitable squeezing, their crystal structures can be distorted to ones that can sustain a dipole moment. Such crystals are called *piezoelectric*. The point group of a piezoelectric crystal (when unstrained) cannot contain the inversion.

## FERROELECTRICITY

The most stable structure of some crystals is nonpyroelectric above a certain temperature  $T_c$  (known as the *Curie temperature*) and pyroelectric below it.<sup>30</sup> Such crystals (examples are given in Table 27.4) are called ferroelectrics.<sup>31</sup> The transition from the unpolarized to the pyroelectric state is called first order if it is discontinuous (i.e., if  $\mathbf{P}$  acquires a nonzero value immediately below  $T_c$ ) and second or higher order, if it is continuous (i.e., if  $\mathbf{P}$  grows continuously from zero as  $T$  drops below  $T_c$ ).<sup>32</sup>

Just below the Curie temperature (for a continuous ferroelectric transition) the distortion of the primitive cell from the unpolarized configuration will be very small, and it is therefore possible, by applying an electric field opposite to this small polarization, to diminish and even reverse it. As  $T$  drops farther below  $T_c$ , the distortion of the cell increases, and very much stronger fields are required to reverse the direction of  $\mathbf{P}$ . This is sometimes taken as the essential attribute of ferroelectrics, which are then defined as pyroelectric crystals whose polarization can be reversed by applying a strong electric field. This is done to include those crystals one feels would satisfy the first definition (existence of a Curie temperature), except that they melt before the conjectured Curie temperature can be reached. Well below the Curie temperature, however, the reversal of polarization may require so drastic a restructuring of the crystal as to be impossible even in the strongest attainable fields.

Immediately below the Curie temperature of a continuous ferroelectric transition, the crystal spontaneously and continuously distorts to a polarized state. One would therefore expect the dielectric constant to be anomalously large in the neighborhood of  $T_c$ , reflecting the fact that it requires very little applied field to alter substantially the displacement polarization of the crystal. Dielectric constants as large as  $10^5$  have been observed near ferroelectric transition points. In an ideal experiment the dielectric constant should actually become infinite precisely at  $T_c$ . For a continuous transition this simply expresses the fact that as  $T_c$  is approached from above, the net restoring force opposing a lattice distortion from the unpolarized to the polarized phase vanishes.

If the restoring force opposing a particular lattice distortion vanishes, there should be a zero-frequency normal mode whose polarization vectors describe precisely this distortion. Since the distortion leads to a net dipole moment and therefore involves a relative displacement between ions of opposite charge, the mode will be an optical mode. In the vicinity of the transition, relative displacements will be large, anharmonic terms will be substantial, and this "soft" mode should be rather strongly damped.

These two observations (infinite static dielectric constant and a zero-frequency optical mode) are not independent. One implies the other by the Lyddane-Sachs-Teller relation (27.67), which requires the transverse optical-mode frequency to vanish whenever the static dielectric constant is infinite.

<sup>30</sup> Transitions back and forth are also known: e.g., there can be a range of temperatures for the pyroelectric phase, above and below which the crystal is unpolarized.

<sup>31</sup> The name stresses the analogy with ferromagnetic materials, which have a net *magnetic* moment. It is not meant to suggest that iron has any special relation to the phenomenon.

<sup>32</sup> Sometimes the term "ferroelectric" is reserved for crystals in which the transition is second order.

Perhaps the simplest type of ferroelectric crystal (and the one most widely studied) is the perovskite structure, shown in Figure 27.10. Other ferroelectrics tend to be substantially more complex. Some characteristic examples are given in Table 27.4.

Figure 27.10

The perovskite structure, characteristic of the barium titanate ( $\text{BaTiO}_3$ ) class of ferroelectrics in the unpolarized phase. The crystal is cubic, with  $\text{Ba}^{++}$  ions at the cube corners,  $\text{O}^{--}$  ions at the centers of the cube faces, and  $\text{Ti}^{4+}$  ions at the cube centers. The first transition is to a tetragonal structure, the positive ions being displaced relative to the negative ones, along a  $[100]$  direction. The perovskite structure is an example of a cubic crystal in which every ion is *not* at a point of full cubic symmetry. (The  $\text{Ba}^{++}$  and  $\text{Ti}^{4+}$  are, but the  $\text{O}^{--}$  ions are not.) Therefore the local field acting on the oxygen ions is more complicated than that given by the simple Lorentz formula. This is important in understanding the mechanism for the ferroelectricity.

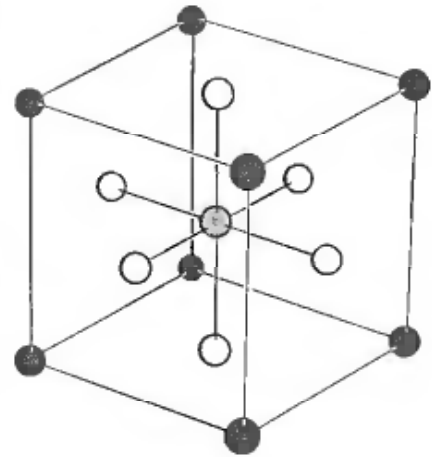


Table 27.4

SELECTED FERROELECTRIC CRYSTALS

NAME	FORMULA	$T_c$ (K)	$P$ ( $\mu\text{C}/\text{cm}^2$ )	at $T$ (K)
Potassium dihydrogen phosphate	$\text{KH}_2\text{PO}_4$	123	4.75	96
Potassium dideuterium phosphate	$\text{KD}_2\text{PO}_4$	213	4.83	180
Rubidium dihydrogen phosphate	$\text{RbH}_2\text{PO}_4$	147	5.6	90
Rubidium dideuterium phosphate	$\text{RbD}_2\text{PO}_4$	218	—	—
Barium titanate	$\text{BaTiO}_3$	393	26.0	300
Lead titanate	$\text{PbTiO}_3$	763	> 50	300
Cadmium titanate	$\text{CdTiO}_3$	55	—	—
Potassium niobate	$\text{KNbO}_3$	708	30.0	523
Rochelle salt	$\text{NaKC}_4\text{H}_4\text{O}_6 \cdot 4\text{D}_2\text{O}$	$\left. \begin{matrix} 297 \\ 255 \end{matrix} \right\}^a$	0.25	278
Deuterated Rochelle salt	$\text{NaKC}_4\text{H}_2\text{D}_2\text{O}_6 \cdot 4\text{D}_2\text{O}$	$\left. \begin{matrix} 308 \\ 251 \end{matrix} \right\}^a$	0.35	279

<sup>a</sup> Has upper and lower  $T_c$ .

Source: F. Jona and G. Shirane, *Ferroelectric Crystals*, Pergamon, New York, 1962, p. 389.

## PROBLEMS

### 1. Electric Field of a Neutral Uniformly Polarized Sphere of Radius $a$

Far from the sphere, the potential  $\phi$  will be that of a point dipole of moment  $p = 4\pi Pa^3/3$ :

$$\phi = \frac{P \cos \theta}{r^2}, \quad (27.80)$$

(where the polar axis is along  $\mathbf{P}$ ). Using the fact that the general solution to  $\nabla^2\phi = 0$  proportional to  $\cos\theta$  is

$$\frac{A \cos\theta}{r^2} + Br \cos\theta, \quad (27.81)$$

use the boundary conditions at the surface of the sphere to show that the potential inside the sphere leads to a uniform field  $\mathbf{E} = -4\pi\mathbf{P}/3$ .

## 2. Electric Field of an Array of Identical Dipoles with Identical Orientations, at a Point with Respect to Which the Array Has Cubic Symmetry

The potential at  $\mathbf{r}$  due to the dipole at  $\mathbf{r}'$  is

$$\phi = -\mathbf{p} \cdot \nabla \frac{1}{|\mathbf{r} - \mathbf{r}'|}. \quad (27.82)$$

By applying the restrictions of cubic symmetry to the tensor

$$\sum_{\mathbf{r}'} \nabla_{\mu} \nabla_{\nu} \frac{1}{|\mathbf{r} - \mathbf{r}'|}, \quad (27.83)$$

and noting that  $\nabla^2(1/r) = 0$ ,  $r \neq 0$ , show that  $\mathbf{E}(\mathbf{r})$  must vanish, when the positions  $\mathbf{r}'$  of the dipoles have cubic symmetry about  $\mathbf{r}$ .

## 3. Polarizability of a Single Hydrogen Atom

Suppose an electric field  $\mathbf{E}$  is applied (along the  $x$ -axis) to a hydrogen atom in its ground state with wave function

$$\psi_0 \propto e^{-r/a_0}. \quad (27.84)$$

(a) Assume a trial function for the atom in the field of the form

$$\psi \propto \psi_0(1 + \gamma x) = \psi_0 + \delta\psi, \quad (27.85)$$

and determine  $\gamma$  by minimizing the total energy.

(b) Calculate the polarization

$$p = \int d\mathbf{r} (-e) x (\psi_0 \delta\psi^* + \psi_0^* \delta\psi), \quad (27.86)$$

using the best trial function, and show that this leads to a polarizability  $\alpha = 4a_0^3$ . (The exact answer is  $4.5a_0^3$ .)

## 4. Orientational Polarization

The following situation sometimes arises in pure solids and liquids whose molecules have permanent dipole moments (such as water or ammonia) and also in solids such as ionic crystals with some ions replaced by others with permanent moments (such as  $\text{OH}^-$  in  $\text{KCl}$ ).

(a) An electric field tends to align such molecules; thermal disorder favors misalignment. Using equilibrium statistical mechanics, write down the probability that the dipole makes an angle in the range from  $\theta$  to  $\theta + d\theta$  with the applied field. If there are  $N$  such dipoles of moment  $p$ , show that their total dipole moment in thermal equilibrium is

$$Np\langle \cos\theta \rangle = NpL\left(\frac{pE}{k_B T}\right), \quad (27.87)$$

where  $L(x)$ , the "Langevin function," is given by

$$L(x) = \coth x - \left(\frac{1}{x}\right). \quad (27.88)$$

(b) Typical dipole moments are of order 1 Debye unit ( $10^{-18}$  in esu). Show that for an electric field of order  $10^4$  volts/cm the polarizability at room temperature can be written as

$$\alpha = \frac{p^2}{3k_B T}. \quad (27.89)$$

### 5. Generalized Lyddane-Sachs-Teller Relation

Suppose that the dielectric constant  $\epsilon(\omega)$  does not have a single pole as a function of  $\omega^2$  (as in (27.57)) but has the more general structure:

$$\epsilon(\omega) = A + \sum_{i=1}^n \frac{B_i}{\omega^2 - \omega_i^2}. \quad (27.90)$$

Show directly from (27.90) that the Lyddane-Sachs-Teller relation (27.67) is generalized to

$$\frac{\epsilon_0}{\epsilon_\infty} = \prod \left(\frac{\omega_i^0}{\omega_i}\right)^2, \quad (27.91)$$

where the  $\omega_i^0$  are the frequencies at which  $\epsilon$  vanishes. (*Hint:* Write the condition  $\epsilon = 0$  as an  $n$ th-degree polynomial in  $\omega^2$ , and note that the product of the roots is simply related to the value of the polynomial at  $\omega = 0$ .) What is the significance of the frequencies  $\omega_i$  and  $\omega_i^0$ ?